**ISTANBUL TECHNICAL UNIVERSITY ★ GRADUATE SCHOOL OF SCIENCE ENGINEERING AND TECHNOLOGY**

# INVESTIGATION OF INFRARED PHOSPHORESCENCE PROPERTIES OF CHROMIUM DOPED LANTHANUM GALLOGERMANATE PHOSPHORS SYNTHESIZED BY SOL-GEL METHOD

**M.Sc. THESIS**

**Burcu CAN**

**Department of Metallurgical and Materials Engineering**

**Material Science and Engineering Programme**

**May, 2020**

**ISTANBUL TECHNICAL UNIVERSITY ★ GRADUATE SCHOOL OF SCIENCE ENGINEERING AND TECHNOLOGY**

# INVESTIGATION OF INFRARED PHOSPHORESCENCE PROPERTIES OF CHROMIUM DOPED LANTHANUM GALLOGERMANATE PHOSPHORS SYNTHESIZED BY SOL-GEL METHOD

**M.Sc. THESIS**

**Burcu CAN**
**521161015**

**Department of Metallurgical and Materials Engineering**

**Material Science and Engineering Programme**

**Thesis Advisor: Asst. Prof. Dr. Nuri SOLAK**

**May, 2020**

**ISTANBUL TEKNİK ÜNİVERSİTESİ ★ FEN BİLİMLERİ ENSTİTÜSÜ**

# SOL-JEL YÖNTEMİ İLE SENTEZLENEN KROM KATKILI LANTAN GALOGERMANAT FOSFORLARININ KIZILÖTESİ FOSFORESANS ÖZELLİKLERİNİN İNCELENMESİ

**YÜKSEK LİSANS TEZİ**

**Burcu CAN**
**521161015**

**Metalurji ve Malzeme Mühendisliği Anabilim Dalı**

**Malzeme Bilimi ve Mühendisliği Programı**

**Tez Danışmanı: Dr. Öğr. Üyesi Nuri SOLAK**

**Mayıs, 2020**

Burcu CAN, a M.Sc. student of ITU Graduate School of Science Engineering and Technology student ID 521161015 successfully defended the thesis/dissertation entitled "INVESTIGATION OF INFRARED PHOSPHORESCENCE PROPERTIES OF CHROMIUM DOPED LANTHANUM GALLOGERMANATE PHOSPHORS SYNTHESIZED BY SOL-GEL METHOD", which he/she prepared after fulfilling the requirements specified in the associated legislations, before the jury whose signatures

| | | |
|---|---|---|
| **Thesis Advisor :** | **Asst. Prof. Dr. Nuri SOLAK**<br>İstanbul Technical University | ..... |
| **Jury Members :** | **Assoc. Prof. Dr. Derya DIŞPINAR**<br>Istanbul Technical University | ..... |
| | **Asst. Prof. Dr. Fatma BAYATA**<br>Istanbul Bilgi University | ..... |

**Date of Submission : 4 March 2020**
**Date of Defense : 11 May 2020**

***To my family,***

## FOREWORD

I owe a big thanks to everyone who has been with me throughout my graduate advanture and has always supported me in every respect.

Before anything else; I owe the greatest thanks to my esteemed advisor Asst. Prof. Dr. Nuri SOLAK whom I consider very lucky to have opportunity to work with him, who has always made me feel his support and understanding both professionally and personally. I would like to express my sincere thanks to Prof. Dr. Filiz KARAOSMANOĞLU, who is my greatest supporter for this opportunity to work.

I would like to thank all my friends in the SOLAKs group for their assistance during my studies. But there are four people in this group who helped me to carry out my studies and to conclude. My special and greatful thanks to Esra BİNİCİ, Beyza BAKKAL, Gizem SOYDAN and Selim MEŞE for their guidance and amazing assistance.

I would also like to express my gratitude to all my managers and colleagues at Kastamonu Entegre and Eczacıbaşı Tüketim Ürünleri, who have tried to prevent me from feeling the diffuculties of getting a master's degree while working actively in an industrial company. They always have been my supporter to complete my graduate education and for this purpose they provided me wide opportunities that most companies did not provide.

If people always feel the support and faith of their beloved, there is nothing they cannot be able to achieve. I send my sincere thanks to my dear mother and father who brought me to these days with their sacrifices and perfect love. And Okan, thank you very much for being my greatest source of motivation, for not stopping to believe me for even a second and for encouraging me to believe that I will always succeed.

November 2019

Burcu CAN
(Chemical Engineer)

**TABLE OF CONTENTS**

**Page**

**ABBREVIATIONS**

| | |
|---|---|
| **CA** | **:** Citric Acid |
| **CB** | **:** Conduction Band |
| **EC** | **:** External Conversion |
| **FL** | **:** Fluorescence |
| **IC** | **:** Internal Conversion |
| **ISC** | **:** Intersystem Crossing |
| **LED** | **:** Light Emitting Diode |
| **LGG** | **:** Lanthanum Gallogermanate |
| **LGGC** | **:** Chromium Doped Lanthanum Gallogermanate |
| **LSGG** | **:** Lanthanum Strontium Gallogermanate |
| **NIR** | **:** Near-Infrared |
| **PDP** | **:** Plasma Display Panel |
| **PL** | **:** Photoluminescence |
| **SSR** | **:** Solid State Reaction |
| **UV** | **:** Ultraviolet |
| **VB** | **:** Valence Band |
| **VR** | **:** Vibrational Relaxation |
| **XRD** | **:** X-Ray Diffraction |

**SYMBOLS**

| | |
|---|---|
| **$S_0$, $S_1$, $S_2$** | **:** Singlet energy levels |
| **$T_1$** | **:** Triplet energy level |
| **λ** | **:** Wavelength |
| **t** | **:** Time |
| **θ** | **:** Bragg Angle |
| **$M_w$** | **:** Molecular weight |

**LIST OF TABLES**

**Page**

**LIST OF FIGURES**

**Page**

**INVESTIGATION OF INFRARED PHOSPHORESCENCE PROPERTIES OF CHROMIUM DOPED LANTANUM GALLOGERMANATE PHOSPHORS SYNTHESIZED BY SOL-GEL METHOD**

## SUMMARY

The need to illuminate in which they have lived since the ancient times is one of the most important needs of people in order to facilitate daily life. As a result of the discoveries made over the years and the improvements made based on these, lighting technologies have reached the present level. The process started with the discovery of fire; candles, gas lamps and the invention of the bulb in the end has made human life much easier. Following these pioneering discoveries, technology has advanced significantly and fluorescent lamps have been used as lighting tools. These technological developments have contributed to the improvements of many value-added products such as, light emitting diodes (LEDs), plasma display panels and photoluminescent materials, as well as lighting.

The mechanism of photoluminescence can be explained by two different sub-types , fluorescence and phosphorescence. The working principles of these two mechanisms are separated according to the paths followed by electrons during the transition between energy levels. In fluorescence radiation, electrons complete the excitation and emission steps between singlet energy levels, while in the phosphorescence mechanism these transition occurs between singlet and triplet energy levels. The traps locating between the singlet and the triplet levels capture electrons and ensure long-lasting radiation, which is the main logic of the phosphorescence phenomenon. In the case of photoluminescence, the photons are the source that stimulate electrons to radiate and so this mechanism called as “photo”luminescence. There are also different luminescence mechanisms which are called according to different radiation sources. For instance; heat in “thermo”luminescence, electrical charge in “electro”luminescence, cathode rays in “cathado”luminescence and energy resulting from chemical reactions in “chemi”luminescence direct the electrons to an upper state.

The first appearance of phosphorescence materials took place in Italy in the early $17^{th}$ century. A volcanic stone found by an Italian alchemist was exposed to high temparatures to obtain a metal. However, the heated stone has become a glowing material in the dark, rather than becoming a metal. The name “Bolognian stone” which takes its name from the city where the alchemist lives was the first material in which the self-glare feature in the dark was discoved. Subsequent studies have shown that this stone was in fact $BaS_2$, ie, barite, which undergoes heat treatment into $Ba(SO_4)$. After the illumination mechanism of barium sufide, studies on phosphorescence materials gained importance. ZnS, CaS, SrS are among the most widely stuied phosphors. As a result of the studies, it has been proved that doping with different ions gives positive results for improving the intensity and duration of radiation. Transition metals such as Cu, Co, Cr as well as rare earth elements such as Eu, Dy, Er have been used as doping ions. In phosphors synthesized by co-doping method of these elements to the main matrix, it has been proved that the duration and intensity of radiation are

prolonged. However, due to chemically unstable nature of the sulfide-based materials, it is possible to produce $H_2S$ gas in contact with moisture in the air. Therefore, in the following studies, alkaline earth aluminate based phosphorescence materials have been focused. The most common of these type of phosphors are $SrAl_2O_4$, $CaAl_2O_4$, $BaAl_2O_4$ and many studies have been carried out to improve their afterglow properties by adding rare earth elements to the structure. Owing to their positive features like being chemically stable, having long-term and high intensity radiation in visible emission wavelength (450-530 nm) with bright colours, they have several industrial usage area such as lighting equipments, warning signs, functional paints, etc.

In addition to the phosphors emitting in the visible region, many detailed studies have been conducted on the types of phosphorescence material that emit in the near-infrared (NIR) region. Near-infrared radiating phosphors have started to be used in night vision camera systems with advancing defense technologies or in systems that provide biological imaging of cells and tissues with advances in biomedical field. These materials are generally obtained by adding $Cr^{3+}$ ions to spinal gallate and aluminate or gallogermanate matrices. Also in some studies, radiation intensity and duration were improved by addition of rare earth elements. Due to the ability of $Cr^{3+}$ ion to be replaced by Ga or Al in the matrix, structural defects and electron traps occur in the crystal system. As a result of excitation with the UV source, emission occurs in 700-1300 nm wavelengths. One of the phosphors which emit in the infrared region of the spectrum and have been studied in detail is the materials having the lanthanum gallogermanate matrix. The optimum doping rate of $Cr^{3+}$ and reaction conditions of the main phase structure of lanthanum gallogermanate, which is expressed by the formula $La_3Ga_5GeO_{14}$, are investigated. Highly detailed studies on the effects of different secondary doping elements on the crystal structure and radiation properties are also being conducted.

The most widely used powder synthesis method for the production of phosphorescence materials is the solid state reaction method. In the solid state reaction, which is accepted as the conventional method, oxide forms of the elements to be used as starting materials are used. These powdered materials are subjected to heat treatment after being weighed based on the stoichiometric ratios and grinded. Although it is the most widely used method, it is challenging and difficult to obtain homogeneous grain structure since the solid state reaction involves many milling steps. Sol-gel method, which is another powder synthesis method is much easier, faster and gives better results than the solid state method. In the sol-gel method, the reaction begins with the aqeous solution of nitrate salts selected as starting materials. Then homogeneneous solution loses its water content with heating and transforms into gel form. When the obtained gel is put in an oven at 200 °C, production of powder material is occured. As a result of heat treatment steps such as calcination and sintering, a very small particle size and homogeneous structure is obtained.

In the majority of studies on $La_3Ga_5GeO_{14}$ phosphors, solid state reaction was chosen as the synthesis method. With this study; the luminescence duration, intensity and the crystal structure of samples synthesized using sol-gel method were investigated. $Cr^{3+}$ doping ratio and $Nd^{3+}$, $Gd^{3+}$, $Pr^{3+}$, $Dy^{3+}$ co-doped situations were chosen as the main parameters to be investigated for their effects on phosphorescence properties. Additionally, the impacts of substitution of $La^{3+}$ with $Sr^{2+}$ ion at two different rates and also $Ga^{3+}$ substitution with $Al^{3+}$ and $Mg^{2+}$ ions on afterglow properties were investigated in the following steps of the experimental study. In these studies, firstly, phosphor synthesis was carried out with a $Cr^{3+}$ addition ratio of 0.5%, 1% and 3%.

Subsequently, 1% $Cr^{3+}$ - 1% $Nd^{3+}$/1% $Gd^{3+}$/1% $Pr^{3+}$/1% $Dy^{3+}$ co-doped materials was produced to examine the effect of secondary doping element. After determining the optimum doping rate and co-dopant, $Sr^{2+}$ added to the structure for the substitution of $La^{3+}$, stoichiometrically 0.1 and 0.2. In the last step of the study, $Al^{3+}$ and $Mg^{2+}$ were added to final decided sturucture by substitution of $Ga^{3+}$ at the stoichiometric rate of 1. For the phosphor synthesis, nitrate and acetate compounds of the elements were converted into aqueous solution to form gel at ~100 °C. After obtaining the powder in at 200 °C, calcination was carried out for 6 hours at 800 °C, then sintering was completed for 4 hours at 1300 °C. Before sintering, powder samples were filled into silicone molds and shaped under isostatic press under the 400 MPa pressure. The heat treated samples were characterized by XRD and fluorescence spectrometer and the results were compared.

As a result of the experimental studies and all the characterizations, it was determined that the optimum $Cr^{3+}$ dopant ratio was %1 and the best co-dopant was $Nd^{3+}$ in terms of the emission intensity and decay time. In the second stage of the experimental study, the effects of $Sr^{2+}$ ion, which was added to the structure by substituting a certain amount of $La^{3+}$ ion, were examined and it was found that the amount of substitution with the best afterglow performance was 0.2. In the $Sr^{2+}$ substituted structure, the effects of co-dopants were examined and it was concluded that $Nd^{3+}$ and $Gd^{3+}$ additives had positive effects on the afterglow intensity and decay time. In the last stage, when $Al^{3+}$ and $Mg^{2+}$ elements are added to the structure as a substitute for $Ga^{3+}$ ion, how the phosphorescent properties change was examined. While both of these additives reduced the emisson intensity of the phosphor, the $Al^{3+}$ additive extended the decay time, unlike $Mg^{2+}$. While the emission wavelength of the initial structure, in which the synthesized phosphorus has only $Cr^{3+}$ and co-dopants, was 719 nm, this value changed to 709 nm with the addition of $Sr^{2+}$ and 726 nm with the addition of $Mg^{2+}$.

# SOL-JEL YÖNTEMİ İLE SENTEZLENEN KROM KATKILANDIRILMIŞ LANTAN GALOGERMANAT FOSFORLARININ KIZILÖTESİ FOSFORESANS ÖZELLİKLERİNİN İNCELENMESİ

## ÖZET


Eski çağlardan beri yaşadıkları ortamı aydınlatma ihtiyacı, günlük yaşamı kolaylaştırmak açısından insanların önemli ihtiyaçlarının başında gelmiştir. Yıllar boyunca yapılan keşifler ve bunlardan yola çıkarak yapılan geliştirmeler sonucunca aydınlatma teknolojileri günümüzdeki seviyesine ulaşmıştır. Ateşin keşfedilmesi ile birlikte başlayan bu süreç; mum, gaz lambaları ve sonunda ampulün icat edilmesi ile insan hayatını oldukça kolaylaştırmıştır. Bu öncü keşiflerin ardından günümüze kadar geçen sürede teknoloji ciddi anlamda ilerlemiş ve aydınlatma araçları olarak floresans lambalar kullanılmaya başlamıştır. Bu teknolojik gelişmeler, aydınlatmanın yanı sıra ışık yayan diyotlar (LED), plazma ekranlar ve fotolüminesans malzemeler gibi katma değerli birçok ürünün geliştirilmesine de katkı sağlamıştır.

Fotolüminesans mekanizması iki farklı alt ışıma türü ile açıklanabilir, floresans ve fosforesans. Bu iki alt mekanizmanın çalışma prensipleri, elektronların enerji seviyeleri arasındaki geçiş sırasında izledikleri yollara göre birbirinden ayrılmaktadır. Floresans ışımasında, elektronlar tekli enerji seviyeleri arasında uyarılma ve emisyon basamaklarını tamamlarken, fosforesans mekanizmasında bu geçişler tekli ve üçlü enerji seviyeleri arasında gerçekleşir. Tekli ve üçlü enerji seviyeleri arasında yer alan tuzaklar elektronları yakalayarak ışımanın uzun süreli olmasını sağlar ki bu fosforesans olayının doğasını oluşturur. Fotolüminesans olayında, elektronları ışıma yapacak şekilde uyaran kaynak fotonlardır ve "fotolüminesans" adı buradan gelmektedir. Farklı uyarıcı kaynaklara göre farklı lüminesans mekanizmaları da mevcuttur. Örneğin; termolüminesansta ısı, elektrolüminesansta elektriksel yük, katodolüminesansta katod ışınları, kemilüminesansta ise kimyasal reaksiyon sonucu ortaya çıkan enerji elektronların uyarılarak bir üst enerji seviyesine çıkmasını ve sonrasında ışıma yaparak başlangıç seviyesine dönmesini sağlar.

Fosforesans malzemelerin ilk ortaya çıkışı 17. yy başlarında İtalya'da gerçekleşmiştir. İtalyan bir simyacı tarafından bulunan bir volkanik taş, metal elde edebilmek amacıyla yüksek sıcaklığa maruz bırakılmıştır. Ancak ısıtılan taş metale dönüşmek yerine, karanlıkta parlayan bir malzeme haline gelmiştir. İsmini simyacının yaşadığı şehirden alan "Bolonya taşı", karanlıkta kendi kendine parlama özelliğinin ilk keşfedildiği malzeme olmuştur. Sonrasında yapılan çalışmalar göstermiştir ki, bu taş aslında ısıl işlem altında $Ba(SO_4)$ bileşiğine dönüşen, $BaS_2$, yani barittir. Baryum sülfitin ışıma mekanizmasının aydınlatılmasından sonra, fosforesans malzemeler ile ilgili çalışmalar önem kazanmıştır. Sülfit bazlı fosforesans malzemelerden ZnS, CaS, SrS, en yaygın olarak çalışılan fosforlardır. Yapılan çalışmalar sonucunda ışıma şiddetinin ve süresinin iyileştirilmesi için yapıya farklı iyonlar ile katkılandırma yapmanın olumlu sonuçlar verdiği kanıtlanmıştır. Cu, Co, Cr gibi geçiş metallerinin yanı sıra, Eu, Dy, Er gibi nadir toprak elementleri de katkılandırma iyonu olarak kullanılmıştır. Bu elementlerin ana matrise çift katkılandırma yöntemi ile sentezlenen fosforlarda, ışıma

süresi ve şiddetinin uzadığı kanıtlanmıştır. Ancak, sülfit bazlı malzemelerin kimyasal olarak kararsız yapıları nedeniyle, havadaki nem ile temas ettiğinde $H_2S$ gazı ortaya çıkarması söz konusudur. Bu nedenle, ilerleyen çalışmalarda toprak alkali aluminat bazlı fosforesans malzemelere yoğunlaşılmıştır. Bu malzemelerden en yaygın olanları $SrAl_2O_4$, $CaAl_2O_4$, $BaAl_2O_2$ gibi fosforlardır ve bunlar da nadir toprak elementleri ile katkılandırılarak fosforesans özelliklerinin iyileştirilmesi ile ilgili birçok çalışma yapılmıştır. Kimyasal olarak kararlı olmaları, uzun süreli ve yüksek şiddette ışıma yapmaları, görünür bölgede (450-530 nm), parlak ve net renkte ışık yaymaları gibi olumlu özellikleri sayesinde birçok kullanım alanı ortaya çıkmıştır. Aydınlatma ekipmanları, uyarı levhaları, fonksiyonel boyalar gibi bir çok endüstriyel alanda kullanımı mevcuttur.

Görünür bölgede ışıma yapan fosforların yanı sıra, kızılötesi bölgede ışıma yapan fosforesans malzeme türleri üzerine son yıllarda birçok detaylı çalışma yürütülmektedir. Gelişen savunma teknolojileri ile birlikte gece görüş kamera sistemlerinde veya biyomedikal alanındaki ilerlemelerle birlikte hücre ve dokuların biyolojik olarak görüntülenmesini sağlayan sistemlerde, kızıl ötesi ışıma yapan fosforlar kullanılmaya başlanmıştır. Bu malzemeler genellikle spinal galat ve aluminat veya galogermanat matrislerine $Cr^{3+}$ iyonu katkılandırılarak elde edilir. Bazı çalışmalarda nadir toprak elementleri ile katkılandırma da yapılarak ışıma şiddeti ve süresi iyileştirilmiştir. Bu tip malzemelerde $Cr^{3+}$ iyonunun, yapıdaki Ga veya Al ile yer değiştirme kabiliyeti sayesinde matriste yapısal hatalar ve electron tuzakları oluşur. UV dalga boylarında gerçekleşen bir uyarılma sonucunda 700-1300 nm dalga boylarında ışıma gerçekleşir. Spektrumun kızılötesi bölgesinde ışıma yapan ve üzerinde oldukça detaylı çalışmaların yapıldığı fosforlardan biri Lantan galogermanat ana matrisine sahip malzemelerdir. Genellikle $La_3Ga_5GeO_{14}$ formülü ile ifade edilen faz yapısı $Cr^{3+}$ katkılandırma çalışmalarında optimum katkı oranı ve reaksiyon koşulları incelenmektedir. Farklı ikincil katkılandırma elementlerinin kristal yapıya ve ışıma özelliklerine olan etkileri üzerine de oldukça detaylı çalışmalar yürütülmektedir.

Fosforesans malzemelerin üretimi için bilinen toz sentez yöntemleri içerisinde en yaygın olarak kullanılanı katı hal reaksiyonu yöntemidir. Geleneksel yöntem olarak Kabul edilen katı hal reaksiyonunda, başlangıç hammaddeleri olarak yapıya girecek elementlerin oksit formları kullanılmaktadır. Bu toz malzemeler belirlenen formüle istinaden strokiyometrik oranlarda tartılarak öğütme işleminden geçirildikten sonra ısıl işlemlere tabii tutulmaktadır. En yaygın kullanılan yöntem olmasına rağmen, katı hal reaksiyonu çok fazla öğütme aşaması içerdiği için homojen tane yapısı elde etmek zor ve meşakatlidir. Diğer bir toz sentez yöntemi olan sol-jel metodu ise katı hal reaksiyonuna göre oldukça kolay, hızlı ve daha iyi sonuçlar veren bir yöntemdir. Sol-jel metodunda reaksiyon, başlangıç malzemeleri olarak seçilen nitrat tuzlarının sulu çözelti haline getirilmesi ile başlamaktadır. Sonrasında homojen çözelti suyunu kaybedip jel formuna geçerek 200 °C'lik fırında toz sentezi gerçekleşmektedir. Kalsinasyon ve sinterleme gibi ısıl işlem basamakları sonucunda oldukça küçük tane boyutunda ve homojen yapıda toz elde edilmiş olur.

$La_3Ga_5GeO_{14}$ fosforları üzerine yapılan çalışmaların büyük çoğunluğunda sentez yöntemi olarak katı hal reaksiyonu seçilmiştir. Bu çalışma ile; sol-jel metodu kullanılarak sentezlenen $La_3Ga_5GeO_{14}$ fosforlarının uyarılma sonrasındaki ışıma süreleri, yoğunluğu ve kristal yapıları incelenmiştir. Fosforesans özelliklerine olan etkileri incelenecek parametreler olarak $Cr^{3+}$ katkı oranı ve $Nd^{3+}$, $Gd^{3+}$, $Pr^{3+}$, $Dy^3$ iyonları ile çift katkılandırma durumu seçilmiştir. Ayrıca ilerleyen adımlarda, yapıdaki $La^{3+}$ iyonunun $Sr^{2+}$ iyonu ile farklı oranlarda ikame edilmesinin ve sonrasında yapıdaki

$Ga^{3+}$ iyonunun $Al^{3+}$ ve $Mg^{2+}$ iyonları ile ikame edilmesinin fosforesans özellikleri üzerindeki etkileri de incelenmiştir. Yapılan deneysel çalışmalarda, öncelikle $Cr^{3+}$ katkı oranı %0,5, %1 ve %3 olacak şekilde fosfor sentezi gerçekleştirilmiştir. Sonrasında, ikincil katkılandırma elementlerinin etkisini inceleyebilmek için %1 $Cr^{3+}$ katkısı sabit tutularak ikincil katkı elementlerinin oranı da 1% olacak şekilde çift katkılandırılmış malzemelerin üretimi yapılmıştır. Optimum $Cr^{3+}$ katkı oranı ve en etkili ikincil katkı elementleri belirlendikten sonra yapıdaki $La^{3+}$ iyonu 0.1 ve 0.2 oranlarında $Sr^{2+}$ iyonu ile ikame edilerek malzeme sentezleri yapılmıştır. Bu aşamada belirlenen $Cr^{3+}$ oranı ve ikincil katkı elementleri yapıda kullanılmıştır. Fosforesans özelliklerinde iyileşme sağlanan $Sr^{3+}$ katkı oranı belirlendikten sonra ise, yapıdaki $Ga^{3+}$ iyonu $Al^{3+}$ ve $Mg^{2+}$ iyonları ile yapıdaki değerlikleri 1 olacak şekilde ikame edilmiştir. Fosfor sentezleri için elementlerin nitrat ve asetat bileşikleri sulu çözelti haline getirilerek ~100 °C'de jel oluşumu sağlanmıştır. 200 °C'lik fırında toz elde edildikten sonra 800 °C'de 6 saat bekletilerek kalsinasyon, sonrasında 1300 °C'de 4 saat bekletilerek de sinterleme işlemleri tamamlanmıştır. Sinterleme öncesinde toz numuneler silicon kalıplara doldurularak soğuk izostatik preste 180 tonluk basınç altında şekillendirilmiştir. Elde edilen ısıl işlem görmüş numuneler XRD ve floresans spektrofotometre cihazlarında karakterize edilerek sonuçlar karşılaştırılmıştır.

Sonuç olarak, deney numuneleri ışıma şiddeti ile sönümlenme süreleri açısından karakterize edildiğinde, optimum $Cr^{3+}$ katkı oranının %1 olduğu ve en iyi sonuç veren ikincil katkı elementinin ise $Nd^{3+}$ olduğu belirlenmiştir. Deneysel çalışmanın ikinci aşamasında yapıya $La^{3+}$ iyonuna belli oranda ikame edilerek eklenen $Sr^{2+}$ iyonunun etkileri incelenmiş ve ışıma performansının en iyi olduğu ikame miktarının 0.2 olduğu görülmüştür. $Sr^{2+}$ ikameli yapıda da ikincil katkı elementlerinin etkileri incelenmiş, $Nd^{3+}$ ve $Gd^{3+}$ katkılarının ışıma şiddetleri ve sönümlenme sürelerine olumlu etkileri olduğu sonucuna varılmıştır. Son aşamada ise, $Sr^{2+}$ ikame oranı ve optimum katkı elementleri belirlenen yapıya $Ga^{3+}$ iyonuna ikame olarak $Al^{3+}$ ve $Mg^{2+}$ elementleri eklendiğinde fosforesans özelliklerin nasıl değiştiği incelenmiştir. Bu katkıların ikisi de fosforun ışıma şiddetini azaltırken, $Al^{3+}$ katkısı $Mg^{2+}$'dan farklı olarak sönümlenme süresini uzatmıştır. Sentezlenen fosforunun sadece $Cr^{3+}$ ve ikincil katkılarının olduğu başlangıç yapısının emisyon dalgaboyu 719 nm iken, $Sr^{2+}$ ilavesi ile bu değer 709 nm, sonrasında $Mg^{2+}$ ilavesi ile ise 726 nm olarak değişmiştir.

# 1. INTRODUCTION

Since the beginning of human history, lighting has been one of the major needs of human beings. In early eras, people were satisfied their lighting needs by firing wood and this has been followed by torches, candles and gas flames. With the invention of the lighting bulb, human life became much easier and incandescent lamps were widely used over the centuries. In recent years, the lighting technologies have begun to develop towards fluorescent lamps and value added products like light emitting diodes (LED) and plasma display panels (PDP) as the studies progressed about the photoluminescent materials.

People are trying to find solutions for lighting; in fact, there are many natural lighting mechanisms in nature. Some living organisms like planktons, some bacterias and insects can be noticed especially at nights because they can emit light thanks to bioluminescence mechanism. Emitted light results from converted chemical energy by oxidation of organic substances in the organisms' structure. This kind of "self-luminescence" mechanism in nature has inspired people in photoluminescent studies.

Photoluminescent materials not only use in just lighting tools but also use for electronic devices. With evolution of the communication and information technologies, many devices have been developed and the screens of these devices become visible with the human eye thanks to the photoluminescent materials. Based on these developments and the earlier needs, photoluminescent materials have became a crucial topic to be investigate and work on last few decades. Studies have especially focused on increasing intensity of luminescence, high chromatic and chemical stability, brilliant colors, long persistence, enviromentally-friendly phosphors and their synthesis techniques.

The simplest definition of photoluminescence is the light scattering between the excitation of electrons and the return to ground state. This mechanism can be occurred in two different ways such as fluorescence and phosphorescence. In phosphorescence

mechanism, electrons are trapped by the band gaps and the emission of light continues after the excitation source is removed. This is known as “afterglow effect” [1].

There are a lot of studies in the literature aimed to prolong glowing effect by developing long persistent phosphors. Long-lasting phosphor studies first started with the production of sulphite based materials. ZnS and ZnS doping with $Cu^{+}$ and $Co^{2+}$ ions ($ZnS:Cu^{+}$, $ZnS: Cu^{+}, Co^{2+}$) have been used in various operations such as cathode-ray tubes, thin film applications and these studies followed by the synthesis of alkaline-earth sulphite based phosphors like CuS, SrS doping with $Bi^{3+}$, $Eu^{2+}$ or $Ce^{3+}$. Although sulphite based phosphors can be easily excited by the sunlight, they are not too much preferred in industrial applications due to their chemically unstable structures, weak brightness and insufficient persistence effects [2].

When the long persistent phosphors are mentioned, alkaline-earth aluminates distinguished by their various advantages. Especially strontium aluminate based phosphors that doped with $Eu^{2+}$ and $Dy^{3+}$ ions ($SrAl_2O_4:Eu^{2+}, Dy^{3+}$) have long glowing time, bright color and chemically and thermally stable structure. One of the first study on $SrAl_2O_4: Eu^{2+}, Dy^{3+}$ as a new long persistent phosphor has been done by Matsuzawa et al. in 1996 [3]. In the following years, strontium aluminate based phosphor studies based on production techniques and optimisation processes have been progressed; and today, they are widely used in various applications like sensor technologies, PDP and LED screens, warning signs, luminous paints in textile, ceramics and construction.

Apart from the phosphors emitting light in the visible region of the spectrum, there has been several studies about the near-infrared (NIR) light emitted phosphors, as well. As a result of extensive researches and experimental studies, various types of phosphoresence material which radiate at NIR wavelength have been discovered. Although the first studies about the IR emitting phosphors had been studying from 1970s, the major developments are carried out after the 2000s [4]. Spinal materials as $LiGa_5O_8$, $ZnGa_2O_4$, $MgGa_2O_4$, $LiAl_5O_8$ have been stuied and it is discovered that their light emission at meanly 600-800 nm (NIR region) when they doped with $Cr^{3+}$ ions. Gallogermanate based materials have also been investigated according to their structural defects and traps providing persistent NIR emission. $La_3Ga_5GeO_{14}$, $Ca_3Ga_2Ge_3O_{12}$ and $Zn_3Ga_2Ge_2O_{10}$ are the most studied gallogermanates that are doped with $Cr^{3+}$ and co-doped with different rare earth elements like $Nd^{3+}$, $Dy^{3+}$, $Pr^{3+}$, $Gd^{3+}$ or $Yb^{3+}$. These types of phosphors mainly used for medical and military purposes such

as bioimaging applications (in-vitro or in-vivo), night vision cameras, fingermark powders etc [5].

Main aim of this study is to investigate the effects of different $Cr^{3+}$ doping ratios, co-doping with rare earth elements and substituting of main matrix with different ions such as $Sr^{2+}$, $Al^{3+}$ and $Mg^{2+}$ on luminescence properties. Using sol-gel method for phosphor synthesis during these investigations is among the primary objectives of the study. Considering all these parameters, it is aimed to conribute to the literature in terms of dopant and co-dopant effects in structures substituted with different elements since a similar study is not available in the literature.

# 2. LUMINESCENCE

## 2.1 Terminology

The word of “phosphor” was first discovered by Italian alchemist Vincentinus Casciarolo in the beginning of 17$^{th}$ century in Bologna, Italy. He had aimed to obtain a metal by firing a heavy stone which he found at the bottom of a volcano in an oven. However, he has obtained a material that scattering red light in the dark instead of metal. Invented glowing material was named as “Bolognian stone” and after the year of studies, we are know that the stone was barrite ($BaSO_4$) and it has become BaS with heat treatment. After this leading discovery, there had been various studies about the light emitting materials in Europe and the “phosphorescence” word has been derived from “phosphor” with the meaning of persistent light emission after the excitation source is removed [6].

Phosphors are known as luminescence mechanism and studies have been carried out for years. Word of “luminescence” has been derived from a Latin word “lumen” which means light. Luminescence can be described as a light emission phenomenon and it consists of many types of mechanisms such as photoluminescence, thermoluminescence, electroluminescence, cathadoluminescence and chemiluminescence. All these mechanisms are based on light-scattering logic in the presence of a different excitation source [7].

## 2.2 Mechanism of Luminescence

Luminescence mechanism can be divided into two major parts; absorption and emission. When an excitation source such as photons, heat, electrical field or radiation is existed in a place with a luminescent material, the material easily absorbs this energy and the electrons are excited to the upper energy level. Absorbed energy is emitted as light while the electrons returning to ground state from the excited state. The most commonly known type of luminescence is photoluminescence which is excited by

photons and the photoluminescence mechanism consists of fluorescence and phosphorescence emissions according to difference of excited energy levels [8].

In an atom or a molecule, there are two main energy levels as singlet and triplet states caused by the difference of spin configurations and the quantum numbers. Unlike triplet states, spins are in paired and opposite forms in the singlet states, that's why their energies and properties are different from each other. Spin configurations of singlet and triplet states are shown in Figure 2.1 [9].

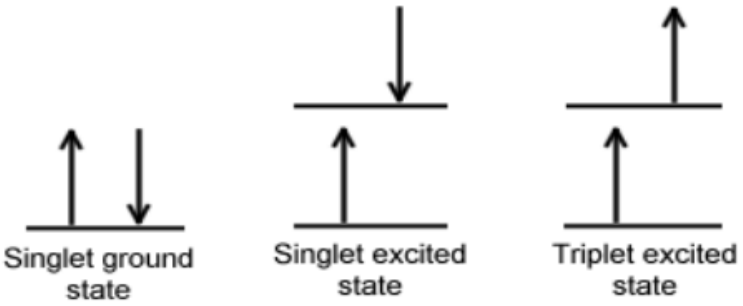


**Figure 2.1 :** Spin configurations of singlet and triplet states.

In some materials, electrons excited from singlet ground state to the singlet excited state and return by following the same route with the identical spin, during which time the light is emitted for a short while. This mechanism is called as "fluorescence". When the excitation and the emission mechanisms occur in between triplet excited state and singlet ground state, it is called as "phosphorescence". In the middle of the excitation and emission processes, there is a random waiting time which is known as relaxation or decay time of an electron. While the relaxation time of fluorescence mechanism is $10^{-5}$-$10^{-8}$ seconds, this time in phosphorescence mechanism can be up to $10^{-4}$-$10^{4}$ seconds. Relaxation mechanism can take place as radiative or non-radiative ways. fluorescence and phosphorescence mechanisms both have radiative relaxation process [10].

Absorption, relaxation and emission processes and the main differences between fluorescence and phosphorescence mechanisms can be understood from the Jablonski diagram that is shown on Figure 2.2 [11].

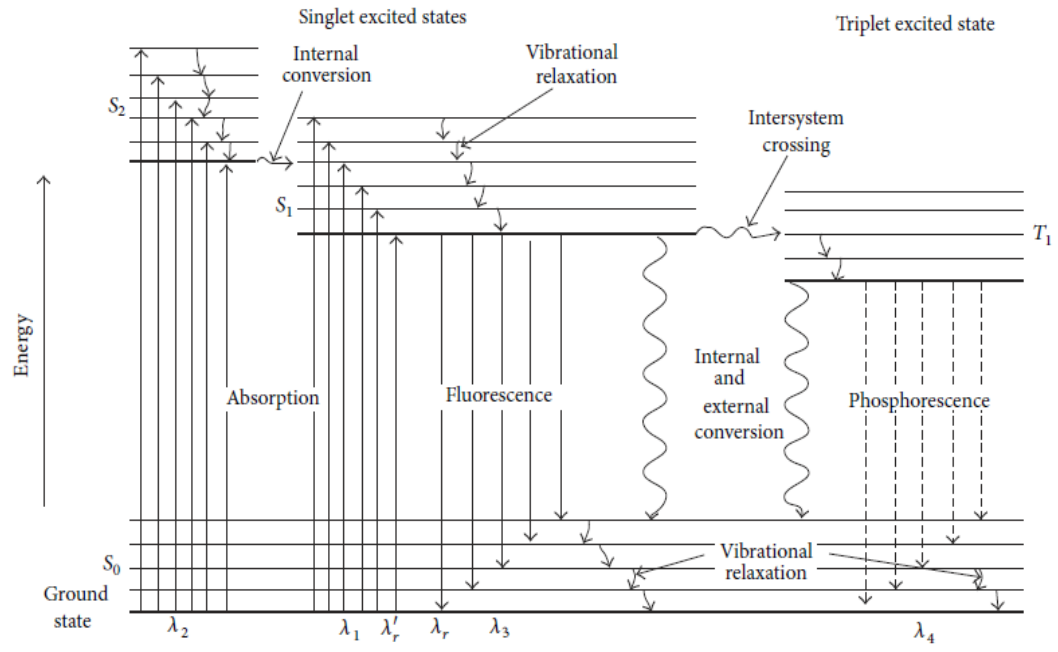


**Figure 2.2 :** Jablonski Diagram.

In the diagram, the horizontal bold lines in the diagram show the vibration energy levels at the bottom of each electronic energy level, while the thin lines indicate the vibration energy levels at each electronic energy level. $S_0$, $S_1$ & $S_2$ and $T_1$ represent singlet ground state, singlet excited states and triplet excited state, respectively. As it shown in the diagram, fluorescence emission happens between $S_0$ and $S_1$ states with the parallel spins. However, in the phosphorescence mechanism, transition tooks place between $S_0$ and $T_1$ which have different spin states. There is always a difference of energy amounts between absorption and emission in both fluorescence and phosphorescence mechanisms. This gap is firstly described by G. Gabriel Stokes in the middle of 19th century and named as “Stokes shift” [12].

Besides the radiative relaxations, there are indicated three types of non-radiative relaxation on the diagram above; internal and extarnal conversion, vibrational relaxation and intersystem crossing. Vibrational relaxation (VR) is a very quick process and caused from energy losing of an electron between the vibrational energy levels in the same electronic state. In this process, vibrational relaxation takes place earlier than emitting of photon and so, the emitted photon comes from the lowest vibrational state. As a different type of non-radiative relaxation, internal conversion (IC) occurs between the energy levels in the same spin. Combination of the internal conversion and the vibrational relaxation gives us the other type of non-radiative

relaxation, external conversion (EC) which takes place without discharging a photon during to return ground state. Finally, when the transition occurs between different spins, this mechanism called as intersystem crossing (ISC) [13].

### 2.3 Classes of Luminescence

Luminescence mechanism has many subdivisions based on the difference of excitation and emission mechanisms and activators. These can be listed as photoluminescence, thermoluminescence, cathadoluminescence, electroluminescence and chemiluminescence.

**Photoluminescence:** It is a type of luminescence that basically relies on the logic of light emitting during to electron transition between different energy levels of a molecule. Electrons are excited by photons and they scattering light in UV visible reagion during return to ground state. According to duration of the relaxation and characteristics of the transition process, photoluminescence mechanism is divided into two subtypes as fluorescence and phosphorescence.

**Thermoluminescence:** An insulator or semiconductor crystal absorbs energy when exposed to ionizing radiation. This absorption leads to the release of some of the electrons in the valence band and to the formation of free electron-gap pairs in the crystal. During the movement of these electrons in the transmission band, the free charge carriers may be recombined with other load carriers with opposite signs or they may be caught by the defect in the crystal and by the load carrier traps formed by the impurities. The trapped electrons remain in the traps for a while depending on the temperature of the medium and the activation energy (trap depth) of the trap level. After removal of the ionizing radiation, the crystal is heated in a controlled manner. During the heating process, the load carriers in the traps can be free from the traps when they gain enough energy and they are free to pass to the transmission band. The released electrons are recombined with counter-labeled load carriers as they move through the crystal, and a luminescence photon is emitted if the reunification event is irradiated. This mechanism is identified as thermoluminescence or thermally stimulated luminescence [14].

**Cathodoluminescence:** Even though the cathodoluminescence mechanism seems like similar to the phosphorescence mechanism, they dissociate from each other in case of

the excitation processes. In cathodoluminescence case, the activators are cathode rays or mobile electrons and the force applied to crystal lattice and atomic shells are higher than the force of photon activators in photoluminescence case. In TVs or some other electronical devices having a screen, cathodoluminescence mechanism is used for the creation of visiual images. [15].

**Electroluminescence:** In electroluminescence mechanism, the role of excitation belongs to the electrical field and it generally happens in semiconductor materials. Excited electrons discharge the energy gained from the electric current as light emission similar to the phosphorescence mechanism [16].

**Chemiluminescence:** When the reaction occurs for forming a new molecule, chemical energy (enthalpy) is released to excite the electrons and this process results in light emission. This mechanism is named as chemiluminescence and it practiced especially on pharmaceutical research about the drug efficiency [11].

Besides the mentioned types of luminescence, there are another subtypes as radioluminescence (activation with X-rays or γ-rays), bioluminescence (activation with biochemical reactions) and triboluminescence (activation with mechanical action).

## 2.4 Long Persistent Phosphors

The word of phosphor means “light bearer” in Greek language and for the centuries significant inventions and numerous studies have been done about the phosphors and their mechanisms. Crystal structure of phosphors includes some certain molecular defects which are caused by the traps related to the own structure of a crystal or the deliberately formed traps in the host or both. Trapped electrons formed by an excitation source and the energy emission by the de-trapping processes provide to occur long persistent emitting of light in UV, VIS or NIR regions of electromagnetic spectrum for minutes up to couple of hours [6].

There are three stages in the phosphoresecence mechanism as it is shown in Figure 2.3; ground state, metastable state and the excited state. In metastable state, electrons or holes are catched by the traps or structural defects and cause the radiative relaxation of electrons.

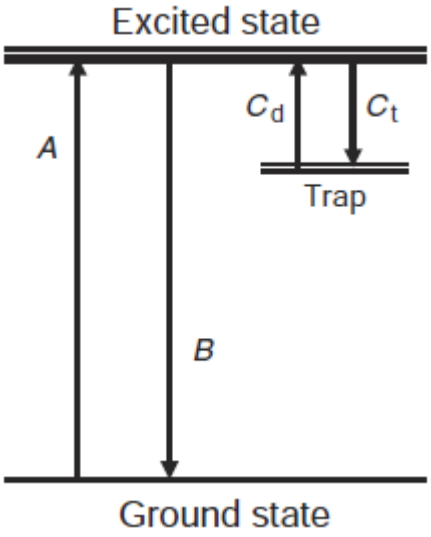


**Figure 2.3 :** Three-level diagram of long persistence mechanism.

The main difference between the phosphoresence and the fluorescence mechanism can be clearly understood from this diagram. While the activation and the emission processes take place only between ground state and excited state (A, B) in fluorescence mechanism, metastable trapping state ($C_d$, $C_t$) is included in phosphorescence mechanism [6].

Structural defects have a role of charge neutralization in the host material. With the replacing ions with each other, a need of charge balance appears and formed gaps will be able to trap a hole or an electron according to dominant charge that needs to be neutralized. Therefore, if the host material or matrix has more defects, more electrons or holes can be captured and duration of phosphorescence will be more. These structural defects are occurred by dislocations or molecular strain resulting from the differences of ionic sizes [17].

Another type of trapping is caused from the co-doping mechanism. Modification with a dopant ion which is in the valence state, creates a metastable state between the valance band an the conduction band for trapping electrons or holes. For example, in $CaS:Eu^{2+}$, $Tm^{3+}$ molecule, $Tm^{2+}$ ion is assumed as a dopant ion which provides forming of traps and taking place of long lasting light emission. Trapping and de-trapping mechanism of $CaS:Eu^{2+}$, $Tm^{3+}$ molecule is shown in Figure 2.4 below.

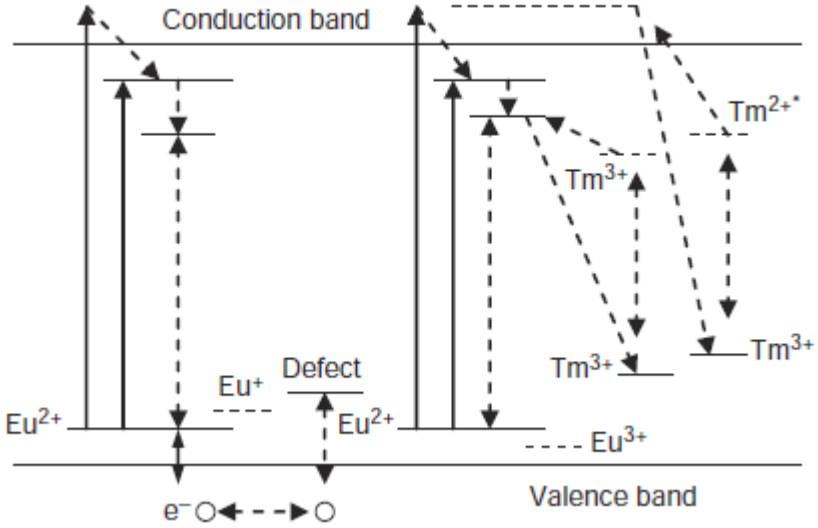


**Figure 2.4 :** Schematic demonstration of trapping and de-trapping process of $CaS:Eu^{2+}$, $Tm^{3+}$ [6].

As the long persistent phosphors, sulphite based phosphors are the most commonly investigated materials for centuries. After the invention of BaS phosphor, CaS, SrS and ZnS phosphors are discovered as a result of long lasting and non-systematic studies. Invention of co-doping with alkaline-earth and rare-earth ions provided to achieve longer emission of light. For example, ZnS is one of the widely used green light emitted long persistent phosphor type and $ZnS:Cu^{+}$ doped material has 40 minutes of light emission after the excitation source is removed. This emitting duration makes doubled by co-doping with $Co^{2+}$ ion and obtained $ZnS:Cu^{+},Co^{2+}$. Likewise, $CaS:Eu^{2+}$ and $SrS:Eu^{2+}$ phosphors have orange-red light emission for a long duration without any co-dopant; however, co-doping with a trivalent ion as $Dy^{3+}$, $Tm^{3+}$ or $Y^{3+}$ prolong to the duration of light emitting [18].

Although sulphite based phosphors have many advantages like long persistent emission or activation with sunlight, their chemically unstable structure and forming of $H_2S$ gas when they exposure to moisture are the main disadvantages of sulphite based phosphors. When viewed from this angle, alkaline-earth aluminate based phosphors like $SrAl_2O_4$, $CaAl_2O_4$ or $BaAl_2O_4$ have better features comparing with the sulphites. Some of the long persistent phosphors are compared in Table 2.1. below according to their compositions and afterglow characteristics after 10 minutes removal of excitation source.

**Table 2.1 :** Luminescence and afterglow features of long persistent phosphors [6].

| Composition | Luminescence color | Luminescence wavelength (nm) | Afterglow brightness ($mcd/m^2$) | Afterglow duration (min) |
|---|---|---|---|---|
| $ZnS:Cu^{+}$ | Yellow-green | 530 | 45 | 200 |
| $ZnS:Cu^{+},Co^{2+}$ | Yellow-green | 530 | 40 | >500 |
| $SrAl_2O_4:Eu^{2+}$ | Green | 520 | 30 | >2000 |
| $SrAl_2O_4:Eu^{2+},Dy^{3+}$ | Green | 520 | 400 | >2000 |
| $Sr_4Al_{14}O_{25}:Eu^{2+},Dy^{3+}$ | Blue-green | 490 | 400 | >2000 |
| $Sr_2MgSi_2O_7:Eu^{2+},Dy^{3+}$ | Blue | 470 | 100 | >1000 |
| $CaS:Eu^{2+},Tm^{3+}$ | Red | 650 | 1.2 | 45 |
| $CaSrS:Bi^{3+}$ | Blue | 450 | 5 | 90 |
| $CaAl_2O_4$: $Eu^{2+},Nd^{3+}$ | Blue | 440 | 35 | >1000 |

Based on the comparison table; although the wavelengths of ZnS and $SrAl_2O_4$ based phosphors are very close to each other, there is a significant difference between their afterglow durations. Thus, strontium aluminate based phosphors commonly investigated and widely used in different industrial applications.

Beginning with the invention of $SrAl_2O_4:Eu^{2+}$ phosphors by Matzusawa et al., investigations about the long persistent phosphors are progressed on alkaline-earth aluminates and their dopants. After the many of studies, it is proved that co-doping with $Dy^{3+}$ ion provides to the much longer afterglow effect and higher luminescence intensity [3].

In the structure of $SrAl_2O_4$ host material, divalent lanthanite ions like $Eu^{2+}$ act like luminescence centers due to the transition of $4f^{n} - 4f^{n-1}5d$ configurations. Trivalent lanthanite ions such as $Dy^{3+}$ have a role of electron trapping in the matrix; herewith, the presence of the both divalent and trivalent lanthanite ions provides to appear long persistence effect of $SrAl_2O_4$: $Eu^{2+}$, $Dy^{3+}$[15].

Although it is not as common as the phosphors emitting light in the visible region, the number of studies on the phosphors emitting in the NIR regions is gradually increasing. Especially in NIR emitting inorganic phosphors, there are some limitations on choosing dopants. Since the dopants generally chosen from rare earth elements, their

very high energy of 5d band and light emissions in visible range may inhibit the NIR emissions. One of the most common dopant for NIR phosphors is $Cr^{3+}$ owing to its proper crystallographic features. Chromium ions can be different valencies such as +1, +2, +3, +5 or +6, but $Cr^{3+}$ valence situation is the most stable and possible one. Furthermore, $Cr^{3+}$ ions have good ability to adjust the crystal structure of the host material and acting as a luminescence center thanks to their changeable energy levels in d electrons with oxygen coordination and crystal field forces. The NIR emission wavelengths can be vary in the range of 700-1300 nm in diverse host materials doping with $Cr^{3+}$. [19].

# 3. NEAR INFRARED PHOSPHORESCENT MATERIALS

## 3.1 Phosphorescent Mechanism of NIR Phosphors

With the progress of the technological advances in the medical and defense industries, the usage areas of the NIR phosphorescence materials have increased. Consequently, the studies about this type of materials have become more important and detailed studies on different host materials, doping and co-doping mechanisms have started. Spinal materials doping with transition metals are one of the most stuied NIR emitting phosphors. Trivalent chromium doped gallate oxides and aluminate oxides such as $LiGa_5O_8$:Cr,$^{3+}$ $ZnGa_2O_4$:$Cr^{3+}$ and $LiAl_5O_8$:$Cr^{3+}$, are some of the most widely stuied NIR phosphors. Their emission wavelength is about in the range of 600-800 nm and the afterglow properties are quite well. Mostly used long persistent NIR phosphors are listed below in Table 3.1 [4].

**Table 3.1 :** Luminescence and afterglow features of NIR phosphors.

| Composition | Activator | Luminescence wavelength (nm) | Afterglow duration (h) |
|---|---|---|---|
| $La_3Ga_5GeO_{14}$ | $Cr^{3+}$ | 700-1300 | >1 - 8 |
| $Zn_3Ga_2Ge_2O_{10}$ | $Cr^{3+}$ | 650-800 | >360 |
| $Sr_3Ga_2Ge_4O_{14}$ | $Cr^{3+}$ | 650-800 | >1 |
| $Ca_3Ga_2Ge_3O_{12}$ | $Cr^{3+}$, $Yb^{3+}$, $Tm^{3+}$ | 650-850 | >1 |
| $LiGa_5O_8$ | $Cr^{3+}$ | 600-850 | >1000 |
| $ZnGa_2O_4$ | $Cr^{3+}$ | 600-800 | >1 |

As can be seen from the table above, gallogermanates are another group of phosphors, which has good NIR phosphorescence properties. After recent studies, it has been proven that the $Cr^{3+}$ ions are the best dopants for NIR phosphors according to their excitation mechanism and electron transition properties.

Figure 3.1 illustrates the NIR emission mechanism resulting from electron transitions between traps and different energy levels of trivalent chromium ions. $^4A_2$ and $^4T_1$ represents the electrons locating in the ground state and in the excited state, respectively.

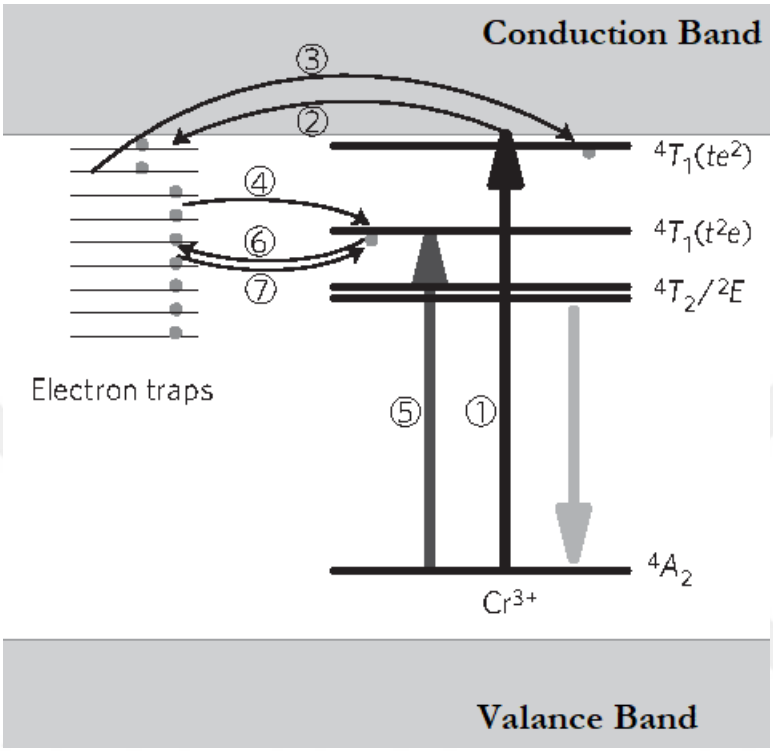


**Figure 3.1 :** Near-infrared emitting mechanism of $Cr^{3+}$ [20].

In the first step of the mechanism (1), $Cr^{+3}$ ions are photoionized by UV source and pass through from the valance band to the conduction band. Electrons progressing in the conduction band are catched by the electron traps (2). De-trapped electron moving reverse direction in the conduction band (3) means the thermal excaping of electrons and recombination with excited Cr ions. This is the beginning of persistent NIR emitting and determine the intensity of emission. Electron transitions representing with (4), (6) and (7) in scheme explain the electron tunnelling mechanism between traps and the triplet excited state $^4T_1(t^2e)$. After a relaxation time between the excited states $^4T_1$ and $^2E$, near infrared emission is occurred with the transition $^4T_1 \rightarrow {}^4A_2$ [19, 21].

### 3.2 Lanthanum Gallogermanate Phosphors

Gallogermanates are remarkable NIR phosphorescence materials which allow to create different host structures based on La, Ca, Zn and to derive many diverse studies by

adding these structures with chromium as a dopant which is a transition metal and different rare earth elements as co-dopants.

Yilling, W. et al (2015) investigated that the effects of different co-dopants on afterglow intensity and persistency of $La_3Ga_5GeO_{14}:Cr^{3+}$ (LGGC) phosphor and they have used $Nd^{3+}$ ion as trivalent co-dopant. With this study, in which the traditional SSR method has been used for synthesis of LGGC, they reported that the co-dopant prolong the afterglow duration and increase the emission intensity when the comparision with the situation of without co-dopants. In Figure 3.2, the emission intensities and decay curves of different doping cases, $La_3Ga_5GeO_{14}:Nd^{3+}$ (LGGN), $La_3Ga_5GeO_{14}:Cr^{3+}$ (LGGC), $La_3Ga_5GeO_{14}:Nd^{3+},Cr^{3+}$ (LGGCN), are shown below. It can be easily observed that the doping with $Cr^{3+}$ ion has the main role of NIR emission and co-doping with $Nd^{3+}$ provides longer and more intense emission [22].

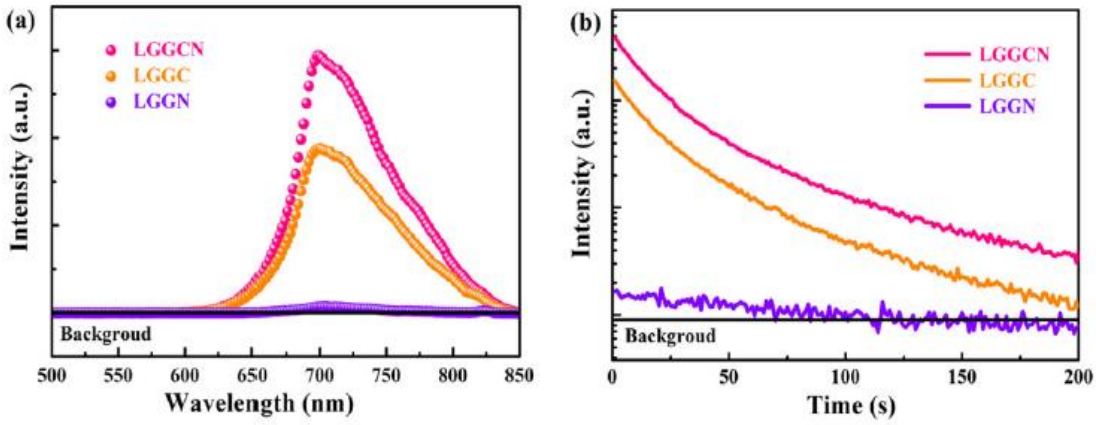


**Figure 3.2 : a)** Afterglow spectra of LGGN, LGGC, LGGCN **(b)** Decay curves of LGGN, LGGC, LGGCN.

In another study, Zhou, J. and Xia, Z. (2013) investigated the variable $Cr^{3+}$ doping ratios on phosphorescence properties of $La_3GaGe_5O_{16}:Cr^{3+}$. They have also used the SSR method for fabrication and tried different $Cr^{3+}$ doping ratios stoichiometrically. NIR Phosphorescence spectrums based on the different concentrations of $Cr^{3+}$ are comperatively shown in Figure 3.3 below. As can be seen from the comparision graph, the optimum doping ratio is 0.03 with the highest intensity observing at 700 nm wavelength, which is NIR emission. After this point, as the stoichiometric ratio of

chromium increase, the emission intensity observing at the same emission wavelength decrease [23].

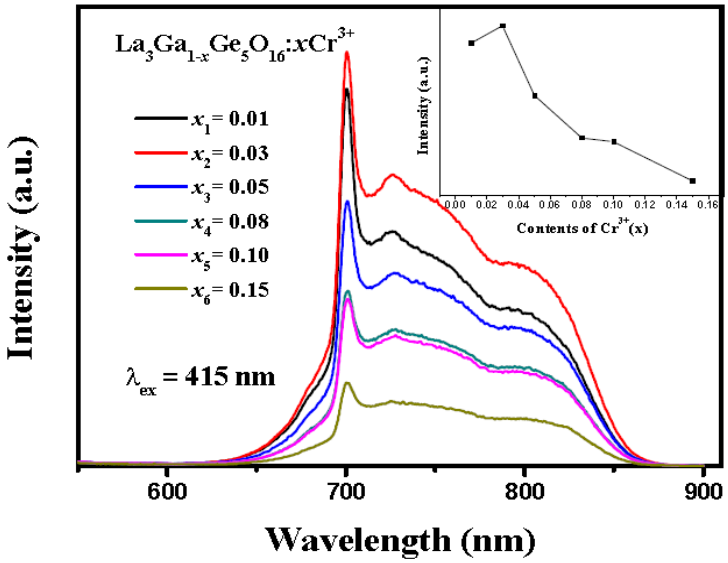


**Figure 3.3 :** Comparision of the emission spectrums based on the different concentrations of $Cr^{3+}$.

### 3.2.1 Crystal Structure

The main reason of choosing $Cr^{3+}$ as a dopant is arised from its capability of substitution to $Ga^{3+}$ ions in disordered octahedrons existing in the crystal structure of lanthanum gallogermanates. $La_3Ga_5GeO_{14}$ has a trigonal crystal system that have $La^{3+}$, $Ga^{3+}$ and $Ga^{3+}$&$Ge^{4+}$ cations in a unit cell, which is shown is shown in Figure 3.4 [24].

A dodecahedron can be seen in the center of the crystal with a La atom placing in the middle of the structure. Ga atoms locating in the site 1a and 3f are situated in an octahedron and a large tetrahedron, respectively. Besides, Ga atom creates a small tetrahedron by sharing its location with Ge atom in the site 2d Dodecahedron and tetrahedrons are surrounded by oxygen ions.

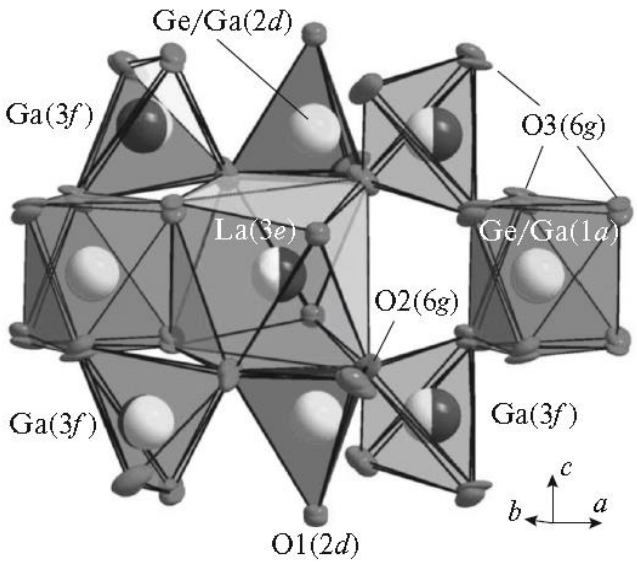


**Figure 3.4 :** Crystal structure of $La_3Ga_5GeO_{14}$ phosphor.

### 3.2.2 Synthesis methods

Synthesis methods of $La_3Ga_5GeO_{14}$: $Cr^{3+}$ phosphors are divided into two main groups as solid state and liquid state techniques. Solid state reaction method is a traditional technique applying from the beginning of phosphorescence studies. Since this method requires high temperature in the reaction and results in a larger particle size, the liquid state reactions made by sol-gel and combustion techniques have become more popular in recent years. Furthermore; hydrothermal, co-precipitation, microemulsion, template method etc. can be listed as the other liquid phase reactions using for fabrication of long persistent phosphors [6].

#### 3.2.2.1 Solid-state reaction

Solid-state reaction (SSR) is known as the most commonly used synthesis method, which performed with powdered form precursors. Generally, starting powder materials are carbonates, oxides and nitrates in certain amounts which calculated by stoichiometric formula. In SSR method, reaction proceeds at high temperatures, because uneven grains of solid precursors need high temperatures to achieve desired phosphorescence effect while sintering. However, the high sintering temperatures

gives rise to relatively large (micrometer sized) and non-uniform particles of final phosphors [25].

$La_2O_3$, $Ga_2O_3$, $GeO_2$ and $Cr_2O_3$ are the conventional precursors and ZnO, $Dy_2O_3$, $Yb_2O_3$, $Er_2O_3$ are the common co-dopants in the synthesis of $La_3Ga_5GeO_{14}$ powders by using SSR technique. Based on the stoichiometry, molar ratios of each compound are calculated and materials are weighed. As a flux material, $H_3BO_3$ or $B_2O_3$ can be added to the system. The reason of this addition is providing better luminescence, obtaining uniform particles and decreasing required temperature of sintering. All of the starting and flux materials are milled and then pre-sintering in air at around 950 °C for 3-5 hours is applied. After repeating the grinding, sintering of acquired powders again for 4-5 hours at around 1200 – 1400 °C in air atmosphere is required to finalize the SSR technique [26].

In the study of Yan, W. et al (2015), it is proven that the LGG phosphor powders which had been obtained by SSR method had NIR phosphorescence emission at in the range of 650 – 850 nm under the excitation of UV lamp at around 250 nm. However, NIR emission was not achieved by blue light excitation at 480 nm wavelength. They have used $Cr_2O_3$ and ZnO precursors in the SSR route as a dopant and co-dopant, respectively [27].

#### 3.2.2.2 Sol-gel method

Sol-gel method is a synthesis technique of ceramic powders and glass materials, which consists of solution - "*sol*" and gelation - "*gel*" stages as the name suggests. The main logic of this technique is forming of a solution, in other words, a suspension with colloidal inorganic particles of precursors such as metal salts or alkoxides and then with the addition of chelating agent, obtaining of three-dimensional matrix as a gel. Gelation arises from covalent bondings between the particles of solution and it is a reversible reaction when the van der Waals and hydrogen bonds are involved to the system [28].

Synthesis of phosphors via sol-gel method has more advantages than the conventional solid-state route in view of the sintering temperatures, controllable microstructure, homogeneously distributed and nano-scale particles. Forming homogeneous gel derives uniform powder grains and highly pure product is obtained because of not to

require milling process. Furthermore, it is an economic and an environmental-friendly technique [29].

To produce $La_3GaGe_5O_{14}$ phosphors by using the sol-gel method, the precursors are generally chosen as the nitrate salts of alkaline-earth and rare-earth elements and acetates of transition metals, such as $La(NO_3)_3$, $Ga(NO_3)_3$, and $Cr_3(OH)_2(OOCH_3)_7$. Besides that, nitrate salt of Ge must be obtained by dissolving of $GeO_2$ in $HNO_3$ solution. However, compared to the solid state reaction method, studies on the synthesis of LGG phosphors using sol-gel technique are relatively inadequate. Therefore, in this study, sol-gel method is used to produce trivalent chromium doped LGG powders.

# 4. EXPERIMENTAL

In this study, the impacts of different $Cr^{3+}$ doping rates and co-doping with different rare-earth elements on the phosphorescence properties of the $La_3Ga_5GeO_{14}$ host material were investigated. In addition, unlike the studies in the literature, it has been studied on the effects of adding elements such as Sr, Al and Mg to the $La_3Ga_5GeO_{14}$ structure on the phosphorescence properties. The samples prepared by following the sol-gel route and according to the determined stoichiometric ratios were characterized after the necessary heat treatments were applied. According to the characterization results, the effects of the investigated parameters on the phosphorescence properties were interpreted.

## 4.1 Preparation of Samples

Based upon the general formula of $La_3Ga_5GeO_{14}$: x% $Cr^{3+}$, LGG samples were prepared by the different ratios of $Cr^{3+}$ dopant over total amount of the samples. Besides; rare earth cations $Dy^{3+}$, $Pr^{3+}$, $Gd^{3+}$ and $Nd^{3+}$ were co-doped to the structure depending on the formulas of $La_3Ga_5GeO_{14}$: x% $Cr^{3+}$, y% $Dy^{3+}$, $La_3Ga_5GeO_{14}$: x% $Cr^{3+}$, y% $Pr^{3+}$, $La_3Ga_5GeO_{14}$: x% $Cr^{3+}$, y% $Gd^{3+}$ and $La_3Ga_5GeO_{14}$: x% $Cr^{3+}$, y% $Nd^{3+}$. Stoichiometric amounts of the precursors were calculated such that the total sample amount for each condition was 2,5 grams. Synthesized samples with the different doping and co-doping rates are given below in the Table 4.1.

**Table 4.1 :** Experimental samples with different doping and co-doping ratios.

| Host Material | % Dopant (x) | % Co-dopant (y) |
|---|---|---|
| $La_3Ga_5GeO_{14}$ | 0.5% $Cr^{3+}$ | - |
| $La_3Ga_5GeO_{14}$ | 1% $Cr^{3+}$ | - |
| $La_3Ga_5GeO_{14}$ | 3% $Cr^{3+}$ | - |
| $La_3Ga_5GeO_{14}$ | 1% $Cr^{3+}$ | 1% $Dy^{3+}$ |
| $La_3Ga_5GeO_{14}$ | 1% $Cr^{3+}$ | 1% $Pr^{3+}$ |
| $La_3Ga_5GeO_{14}$ | 1% $Cr^{3+}$ | 1% $Gd^{3+}$ |
| $La_3Ga_5GeO_{14}$ | 1% $Cr^{3+}$ | 1% $Nd^{3+}$ |

The nitrate and the acetate starting materials with high purity (99,9 %) $La(NO_3)_3$, $Ga(NO_3)_3$, $Cr_3(OH)_2(OOCH_3)_7$ and different nitrate salts of rare earth elements were weighed according to a definite stoichiometric ratio calculated from general formula $La_3Ga_5GeO_{14}$: x% $Cr^{3+}$. $GeO_2$ was dissolved in %65 $HNO_3$ solution to obtain germanium nitrate salt.

Second part of the experimental study was investigation of Sr addition to the LGG matrix by reducing the valance of La in the structure. Modified formula was become $La_{3-z}Sr_zGa_5GeO_{14}$: 1% $Cr^{3+}$ (LSGG) and in the following steps, $Gd^{3+}$ and $Nd^{3+}$ were co-doped into the modified matrix. In Table 4.2, Sr modified formulas and doping ratios of dopants and co-dopants are listed.

**Table 4.2 :** Different rates of Sr addition and co-dopants.

| Host Material | Sr Addition (z) | % Dopant | % Co-dopant |
|---|---|---|---|
| $La_{2.9}Sr_{0.1}Ga_5GeO_{14}$ | 0.1 | 1% $Cr^{3+}$ | - |
| $La_{2.8}Sr_{0.2}Ga_5GeO_{14}$ | 0.2 | 1% $Cr^{3+}$ | - |
| $La_{2.8}Sr_{0.2}Ga_5GeO_{14}$ | 0.2 | 1% $Cr^{3+}$ | 1% $Gd^{3+}$ |
| $La_{2.8}Sr_{0.2}Ga_5GeO_{14}$ | 0.2 | 1% $Cr^{3+}$ | 1% $Nd^{3+}$ |

In the last part of the study, $Al^{3+}$ and $Mg^{2+}$ ions were added to the $La_{2.8}Sr_{0.2}Ga_5GeO_{14}$ main matrix with stoichiometric substitution of Ga. As in the previous studies, 1% $Cr^{3+}$ was added as the dopant and 1% $Nd^{3+}$ was added to the structure as the co-dopant, as well. The final obtained formulas were $La_{2.8}Sr_{0.2}Ga_4AlGeO_{14}$: 1% $Cr^{3+}$, 1% $Nd^{3+}$ and $La_{2.8}Sr_{0.2}Ga_4MgGeO_{14}$: 1% $Cr^{3+}$, 1% $Nd^{3+}$. Al and Mg modified formulas and substitution rates are indicated in Table 4.3.

**Table 4.3 :** Different rates of Sr addition and co-dopants.

| Host Material | Additional Ion | % Dopant | % Co-dopant |
|---|---|---|---|
| $La_{2.8}Sr_{0.2}Ga_4AlGeO_{14}$ | $Al^{3+}$ | 1% $Cr^{3+}$ | 1% $Nd^{3+}$ |
| $La_{2.8}Sr_{0.2}Ga_4MgGeO_{14}$ | $Mg^{2+}$ | 1% $Cr^{3+}$ | 1% $Nd^{3+}$ |

The raw materials used in the synthesis are listed in Table 4.4 with their origins and molecular weights.

**Table 4.4 :** Properties of the raw materials.

| Raw Material | Molecular formula | $M_w$ (g/mole) | Brand (Purity) |
|---|---|---|---|
| Chromium (III) acetate | $Cr_3(OH)_2(OOCH_3)_7$ | 603.31 | Alfa Aesar (99.9%) |
| Magnesium acetate | $Mg(CH_3COO)_2$ | 143.30 | Alfa Aesar (99.9%) |
| Lanthanum nitrate | $La(NO_3)_3$ | 433.01 | Alfa Aesar (99.9%) |
| Strontium nitrate | $Sr(NO_3)_2$ | 211.62 | Alfa Aesar (99.9%) |
| Dysprosium nitrate | $Dy(NO_3)_3$ | 438.59 | Alfa Aesar (99.9%) |
| Praseodymium nitrate | $Pr(NO_3)_3$ | 326.92 | Jiaton (99.9%) |
| Gadolinium nitrate | $Gd(NO_3)_3$ | 451.36 | Jiaton (99.9%) |
| Neodymium nitrate | $Nd(NO_3)_3$ | 438.35 | Jiaton (99.9%) |
| Gallium nitrate | $Ga(NO_3)_3$ | 255.73 | Jiaton (99.9%) |
| Germanium oxide | $GeO_2$ | 104.64 | Jiaton (99.9%) |
| Aluminum nitrate | $Al(NO_3)_2$ | 375.13 | Merck (99.9%) |
| Citric acid | $C_6H_8O_7$ | 210.10 | Merck (99.9%) |

All the precursors were put in a beaker with the adequate amount of distilled water and heated up to 100-105 °C with stable stirring. Since the excess of water will prolong to the time of gelation forming, the amount the water must be adjusted very well. It is important that this procedure is sustained at ~100 °C until getting a perfectly homogeneous solution. After a clear and homogeneous solution was occurred, a certain amount citric acid (CA) that is calculated based upon the total metal ions was used as the cross-linking agent and stirring continued for 2 hours until the solution becomes viscous.

On the next step, fluffy powder material is formed when the gel put in an oven at 200-250 °C for 20-30 min. Then, the residue of carbon is removed by the calcination of powder at 800 - 900 °C for 6 hours occurring in the air atmosphere.

Figure 4.1 shows that the foamy bulk material at the outlet of the drying oven, the first stage in which the powder is obtained. This bulky foam was crushable easily by hands and the powder was ready to calcinate.

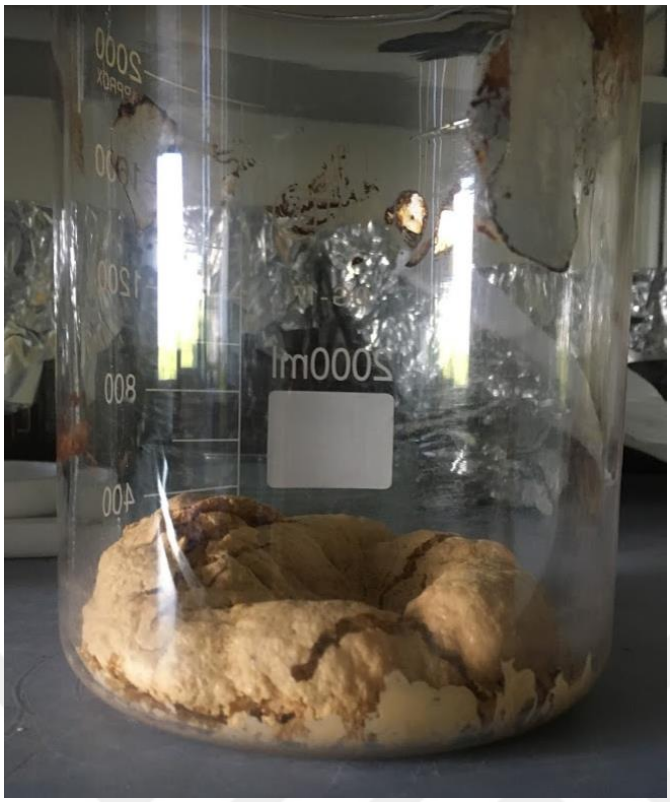

**Figure 4.1 :** Foamy powder after drying in an oven.

Last step in the sol-gel route was the thermal treatment to calcinated LGG powder samples by sintering. Before this operation, the powder samples were shaped by compressed in small silicone molds. Some of the samples of silicone molds filled by the calcinated powders are demonstrated in Figure 4.2.


**Figure 4.2 :** Powder filled silicone molds.

Powder filled silicone molds were pressed in cold isostatic press (CIP) under 180 tons of pressure to obtain compact powder pellets. These pellets were sintered at 1300 °C

for four hours in air atmosphere. Some of the compressed and sintered samples are shown in Figure 4.3. After sintering, colour of the samples has varied from beige to brigth green.


**Figure 4.3 :** Compact powder pellets.

To combine all the experimental steps of LGGC phosphors, a flow chart summarizing the sol-gel technique is indicated below.

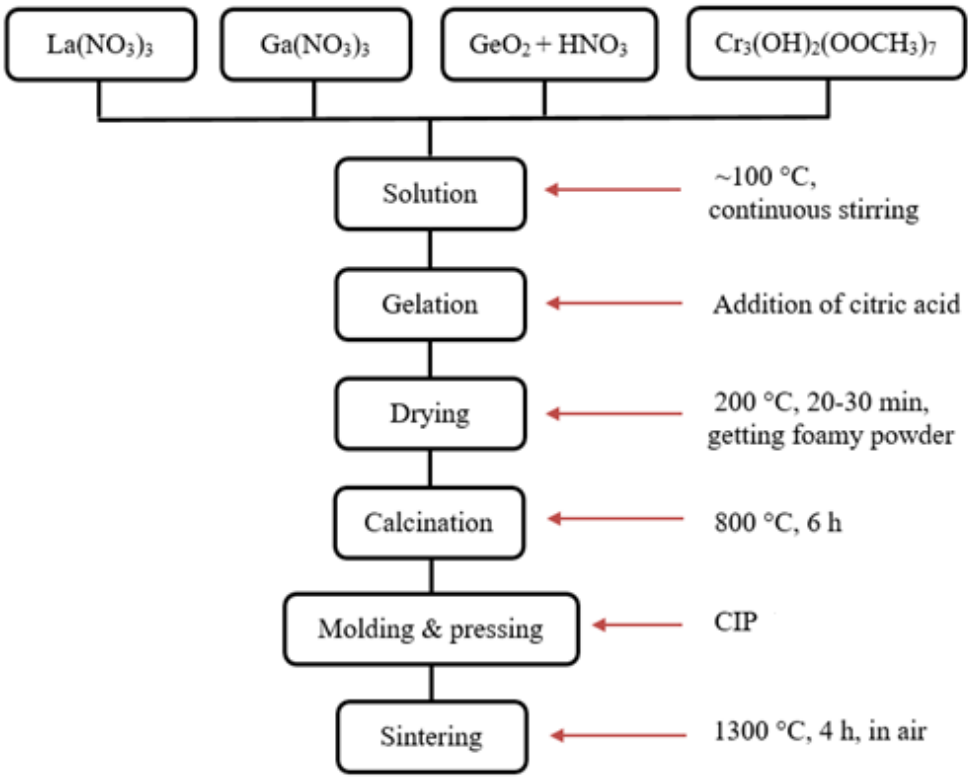


**Figure 4.4 :** Flow chart of the sol-gel synthesis method.

## 4.2 Characterization Methods

### 4.2.1 X-Ray Diffraction (XRD) Analysis

To determine if the correct phases was occurred at the end of the calcination step and to investigate changings in the structure after the sintering step, X-ray diffraction analysis was applied all the LGG and LSGG samples. Results were compared with the JCPDS (Joint Committee on Powder Diffraction Standards) patterns.

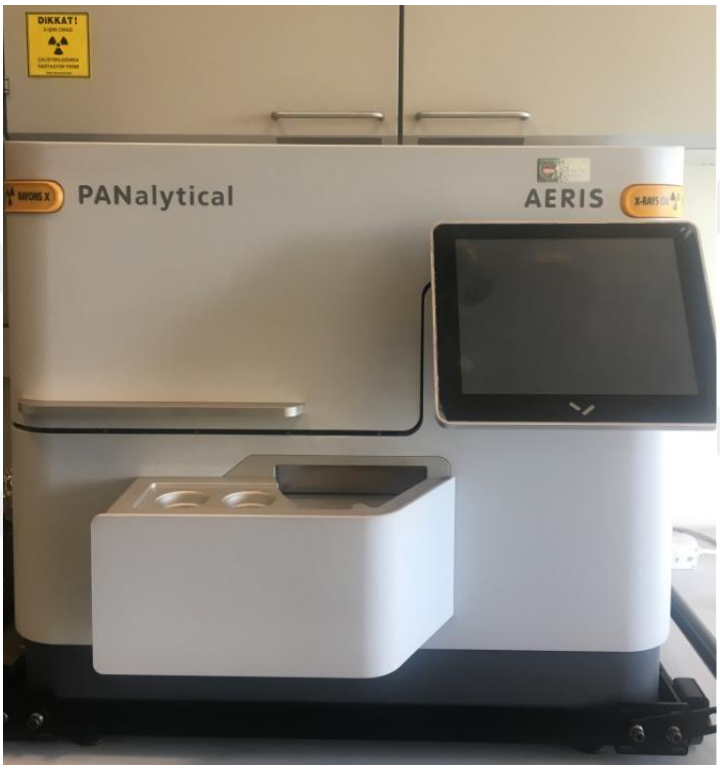


**Figure 4.5 :** XRD PANalytical Aeris.

In this study, X-ray PANalytical Aeris instrument which is demonstrated in Figure 4.4. was used for the characterization using Cu-Kα radiation in the scanning range of 2θ = 10° - 90°.

### 4.2.2 Optical Measurements

Determination of the afterglow properties of samples was done using the modular Ocean Optics - Flame spectrometer. The measurements were taken by fixing the samples to the holder in a black plexiglass box with a 400 µm premium fiber assembly connected to the dedector. Flame spectrometer and the measurement setup are shown in Figure 4.6.

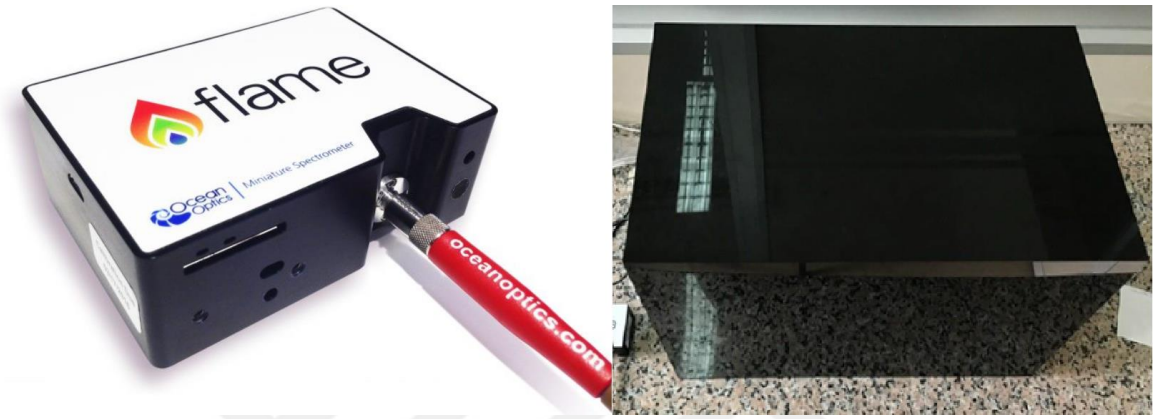


**Figure 4.6 :** Ocean Optics Spectrometer and measurement setup.

Pressed and shaped samples were placed at the same angle to the optical fiber and stimulated with UV source (254 nm) for 1 minute. After excitation, data related to the radiation intensity of the samples were recorded and compared.

In order to compare the decay characteristics, the samples were again stimulated with the UV source (254 nm) for 1 minute. By runnig the device in decay mode, the decay characteristics were obtained as a result of recording rays reaching the device at 1000 ms intervals at the emission wavelengths.

# 5. RESULTS AND DISCUSSIONS

## 5.1 Determination of Optimum $Cr^{3+}$ Doping Ratio

Firstly, in order to examine the effects of different chromium doping ratios on the crystal structure, 0.5%, 1% and 3% $Cr^{3+}$ doped samples were analyzed with X-ray diffractometer after the calcination step (800 °C, 6 h).

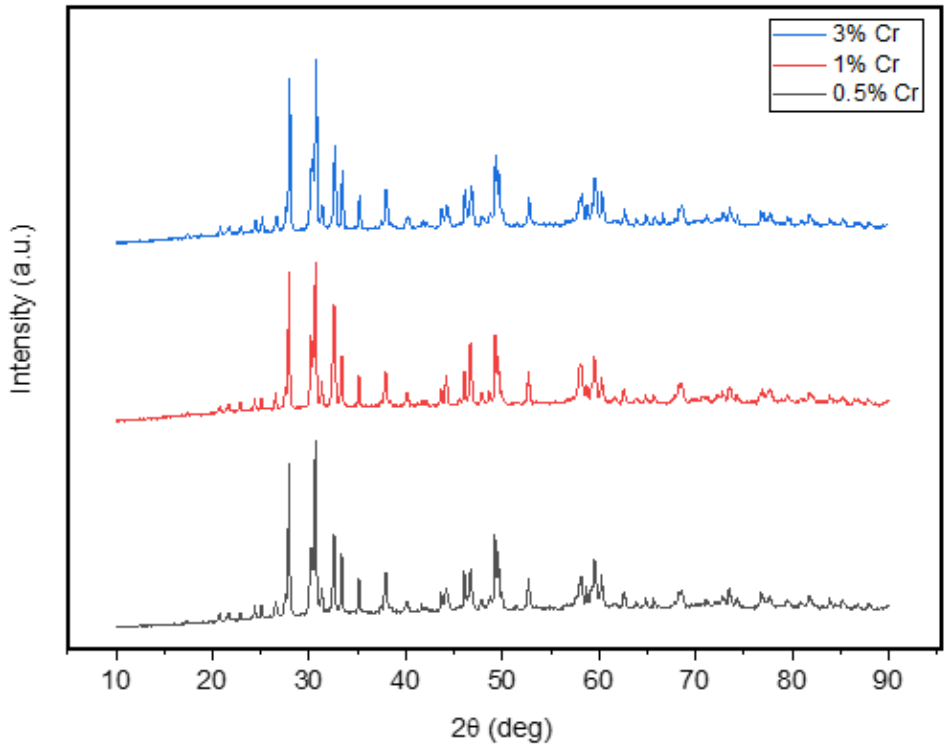


**Figure 5.1 :** XRD patterns of LGG powders based on the different $Cr^{3+}$ doping ratio.

Obtained XRD patterns of the powder samples are given in the Figure 5.1. As seen in the figure, the calcination temperature of 800 °C was sufficient for LGG powders to show crystal structure. XRD patterns of the powders were found to be coherent with the $La_3Ga_5GeO_{14}$ phase expressed by JCPDS #72-2464 when compared with the data from the literature.

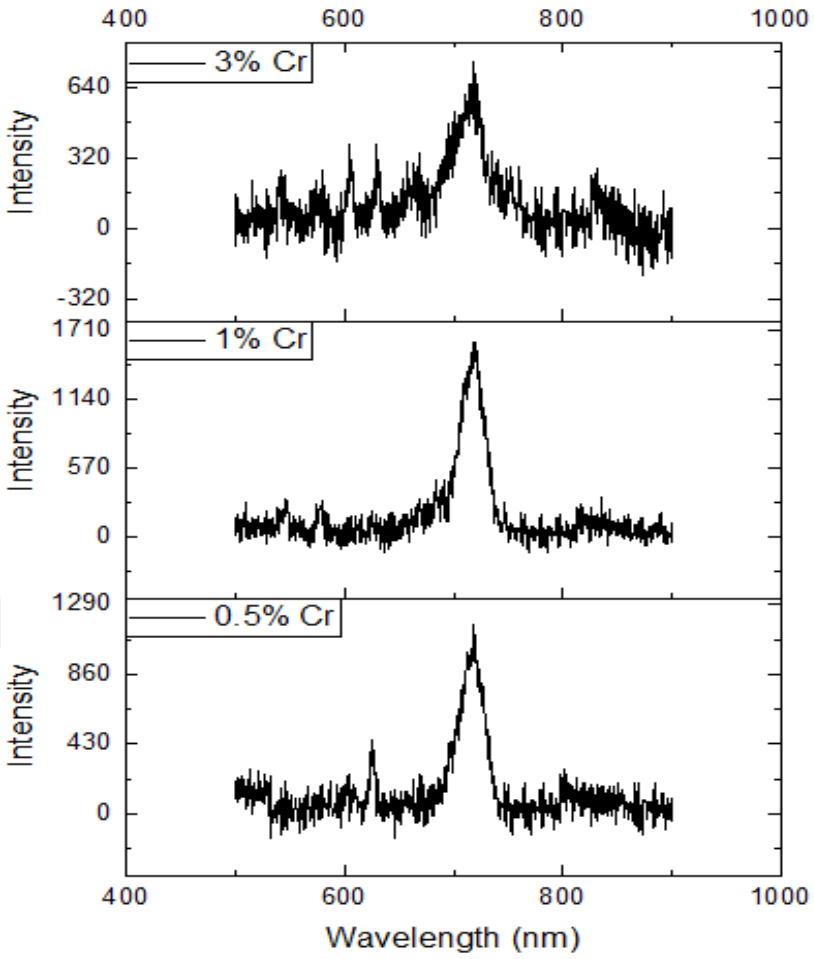


**Figure 5.2 :** Comparision of afterglow intensities of the sintered samples based on the different $Cr^{3+}$ doping ratio.

In Figure 5.2, afterglow intensities of the samples, which doped by $Cr^{3+}$ at three different ratios, were compared. It is obvious that, LGGC powders have emission peaks at approximately 719 nm, which means NIR emission has been occurred. 0.5% and 1% doped samples have sharper emission peaks at 719 nm, but the highest intensity was obtained while the $Cr^{3+}$ doping rate was 1%. For the sample doping 3% $Cr^{3+}$, it can be indicated that the afterglow intensity decreased and this may be resulted from occurring of quenching situation when the doping ratio exceeds a certain value. Possible reasons of the quenching as follows;

- Loss of radiation energy due to cross-relaxation between activators (dopant ions),
- Increased resonance between activators due to increased concentration and thus occurring excitation migration.

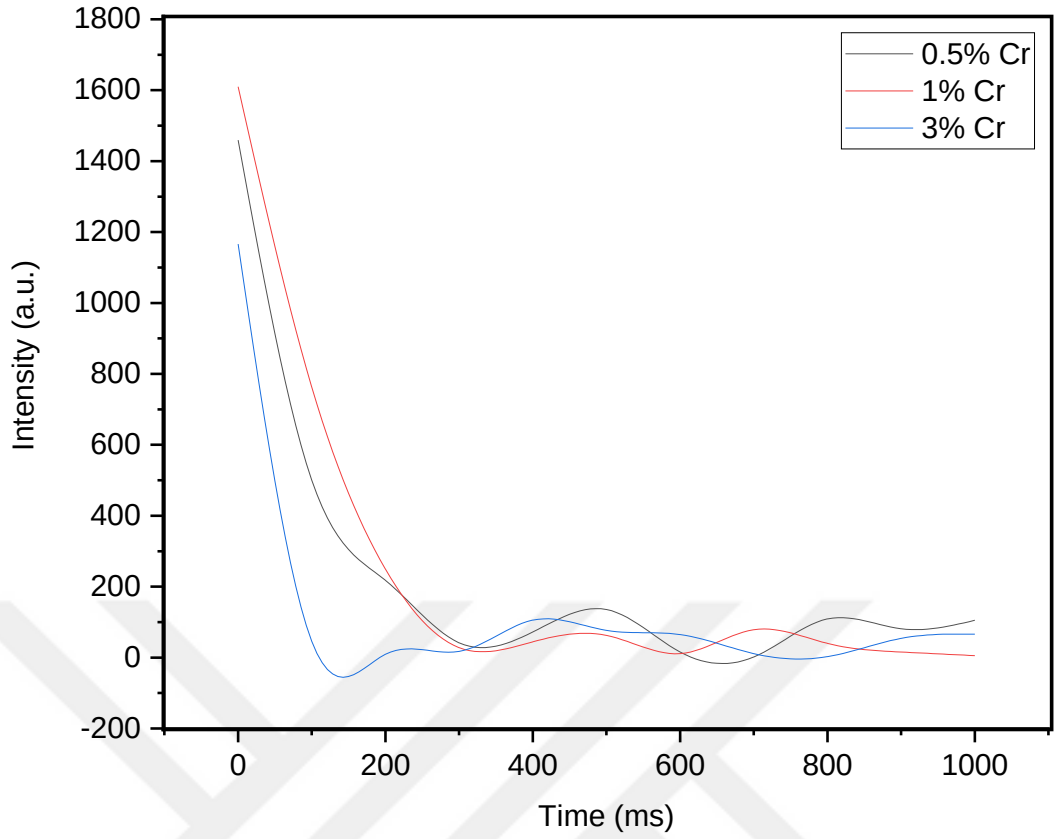


**Figure 5.3 :** Comparision of decay curves of the sintered samples based on the different $Cr^{3+}$ doping ratio.

Decay profiles of the samples were also compared in Figure 5.3. To confirm the quenching explanations above, 3% $Cr^{3+}$ doped LGGC has the lowest decay profile comparing with other samples. The best decay profile is obtained with the 1% doped sample. Therefore, in the following steps of the study, 1% has been chosen as the $Cr^{3+}$ doping rate.

## 5.2 Effects of Different Co-dopants

In the second part of the experimental study, $Dy^{3+}$, $Pr^{3+}$, $Gd^{3+}$ and $Nd^{3+}$ were used as co-dopants together with the same doping rate of $Cr^{3+}$. Since the highest intensity and the best decay profile have been seen in the sample doped by 1% $Cr^{3+}$, co-doped samples were prepared in this part of the study at the rate of 1%.

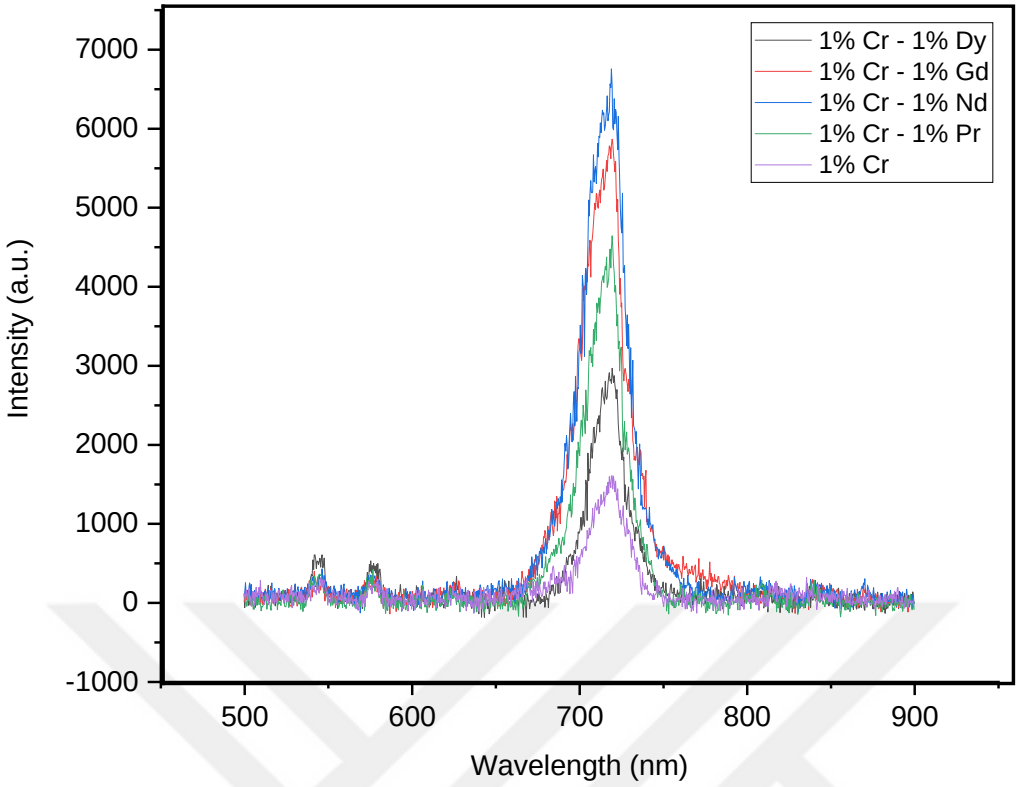


**Figure 5.4 :** Comparision of afterglow properties of 1% $Cr^{3+}$ doped and 1% $Cr^{3+}$- 1% $Dy^{3+}$, $Pr^{3+}$, $Gd^{3+}$ and $Nd^{3+}$ co-doped samples.

Emission peaks and their intensities of co-doped LGGC samples, obtaining after exciting with UV source, were shown in Figure 5.4. As a comparision, the intensity of the emission peaks increased significantly in the case of co-doping with 1% rate of $Dy^{3+}$, $Pr^{3+}$, $Gd^{3+}$ and $Nd^{3+}$. While the $Nd^{3+}$ co-doped sample has the highest emission intensiy, the $Gd^{3+}$ co-doped sample has also relatively intense emission. Although $Pr^{3+}$ and $Dy^{3+}$ have increased the afterglow intensity less than other co-dopants, it was clearly seen that they provide higher intensity than the without co-dopant situation. Emission intensity differences between co-doped LGGC samples are due to the different trap energies of different rare earth elements. Besides, it is obvious that the wavelength of the emission peaks on the graph, has not been affected from addition co-dopants to the LGGC structure. All the emission peaks were observed at 719 nm which is in the NIR region of the spectrum.

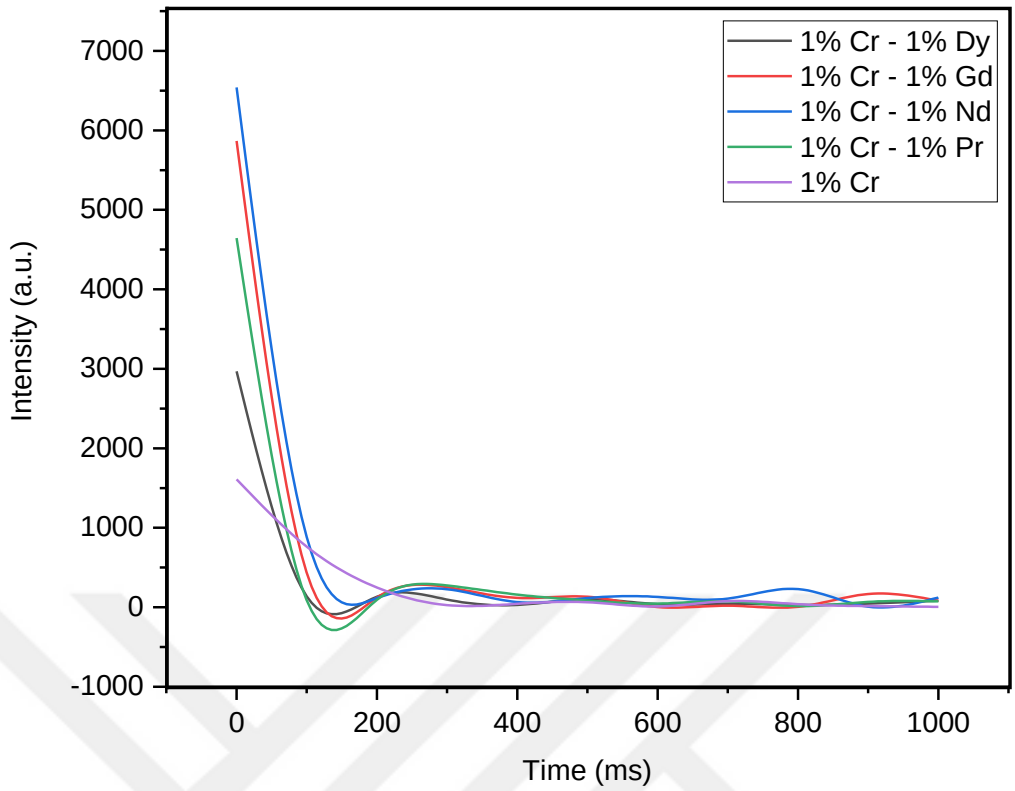


**Figure 5.5 :** Comparision of decay curves of 1% $Cr^{3+}$ doped and 1% $Cr^{3+}$- 1% $Dy^{3+}$, $Pr^{3+}$, $Gd^{3+}$ and $Nd^{3+}$ co-doped samples.

It can be seen from the comparision of decay curves of co-doped samples in Figure 5.5, co-doping mechanism has positive effects on decay times of lanthanum gallogermanate phosphors. This situation is caused from the created traps between singlet and triplet states by co-dopants. The captured electrons by these traps emit light longer during returning to the ground state from the excited state. According to the graph, co-doped sample with $Nd^{3+}$ was showed the best decay profile and $Gd^{3+}$ doped followed to it.

In Figure 5.6, XRD patterns of co-doped LGGC powders that obtained after the sintering step of the sol-gel route have been compared. When the $Dy^{3+}$, $Pr^{3+}$, $Gd^{3+}$ and $Nd^{3+}$ were added to the structure, the single phase structure was intact and compatible XRD patterns with the JCPDS #72-2464 were obtained.

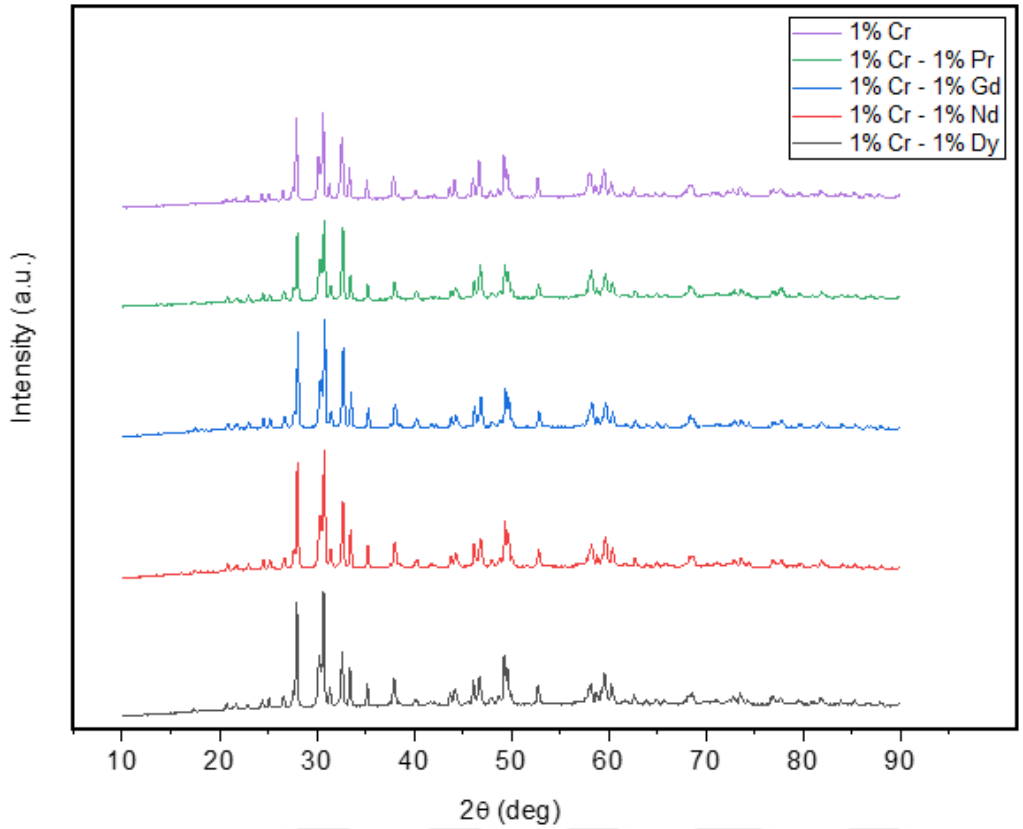


**Figure 5.6 :** Comparision of XRD patterns of 1% $Cr^{3+}$ doped and 1% $Cr^{3+}$- 1% $Dy^{3+}$, $Pr^{3+}$, $Gd^{3+}$ and $Nd^{3+}$ co-doped samples.

### 5.3 Effects of $La^{3+}$ Substitution with $Sr^{2+}$ at Different Ratios

In literature, NIR afterglow properties of strontium gallogermanate phosphors had been studied and it is reported that $Cr^{3+}$ doped $Sr_3Ga_2Ge_4O_{14}$ phosphor was given emission spectrum at around 650-700 nm [30]. However, there is no similar study in the literature about the integration of Sr element into the LGG structure. Therefore, after determining the optimum $Cr^{3+}$ dopant ratio and the most effective co-dopants in the previous steps of the experimental study, the effects of $Sr^{2+}$ substitution made at different rates on $La^{3+}$ ion in the main matrix were investigated. 0.1 and 0.2 were determined as the substitution rate and the general formulas of the LSGG samples were become $La_{2.9}Sr_{0.1}Ga_5GeO_{14}$ and $La_{2.8}Sr_{0.2}Ga_5GeO_{14}$, respectively. While synthesizing the $Sr^{2+}$ substituted samples, $Cr^{3+}$ dopant ratio was kept at 1%.

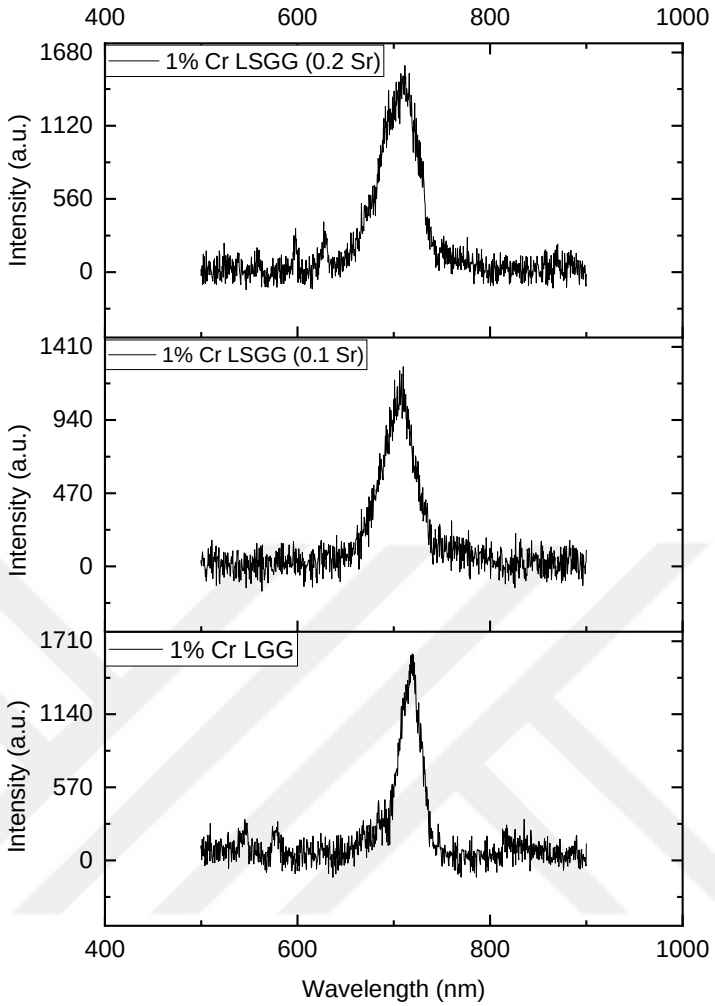


**Figure 5.7 :** Comparision of the afterglow properties of different rate of $Sr^{2+}$ substitution.

When the emission peaks were compared in Figure 5.7, it was seen that 0.2 rate of $Sr^{2+}$ substitution contributed to increase emission intensity. However, the same rise was not observed in the case of 0.1 substitution rate, on the contrary the intensity decreased in this case. Another conclusion understanding from the Figure 5.7 is that the emission wavelength was shifted from 719 nm to 709 nm when the $Sr^{2+}$ ion added to the matrix. It means that added $Sr^{2+}$ ion to the structure changed the energy band gap of the main matrix.

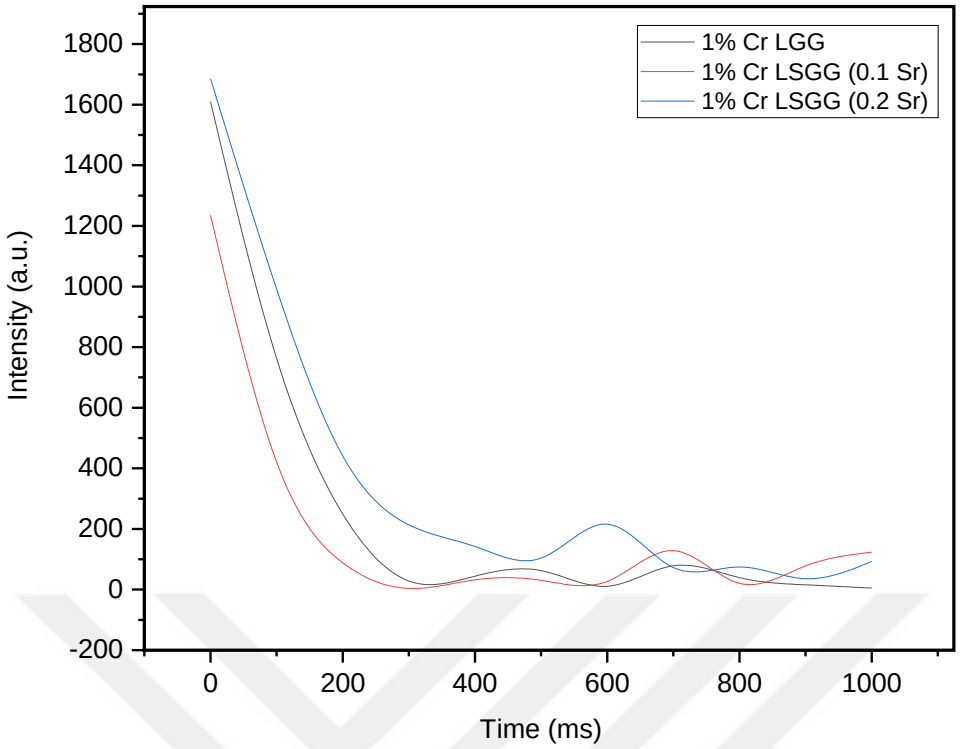


**Figure 5.8 :** Comparision of the decay times of the samples substituting different rate of $Sr^{2+}$.

In Figure 5.8, decay time of substituted sample at the rate of 0.2 is longer than 0.1 substituted and without substitution case. What the reason of the longest emission with 0.2 substitution may be the structural defects acting like traps for catching the electrons and prolonging the emission duration. Thus, in the following steps, 0.2 rate of substitution has been chosen as main matrix with the $La_{2.8}Sr_{0.2}Ga_5GeO_{14}$ formula and it abbreviated as LSGG on the figures.

After this experimental step, the $Nd^{3+}$ and $Gd^{3+}$ co-dopants, which had positive effects on the phosphoresence mechanism, were added to the 0.2 $Sr^{2+}$ substituted structure and their phosphorescence properties were re-examined. Besides, the emission intensities, wavelength and decay profiles of co-doped and without co-dopant LGG and LSGG phosphors. Again in this comparision, $Cr^{3+}$ main dopant ratio of all the samples was kept at 1%. In Figure 5.9, it is obvious that the addition of $Nd^{3+}$ or $Gd^{3+}$ to the $Sr^{2+}$ substituted matrix as a co-dopant increased the afterglow intensity, significantly. The afterglow emission wavelength was remain constant at 709 nm when the co-dopants were added to the structure.

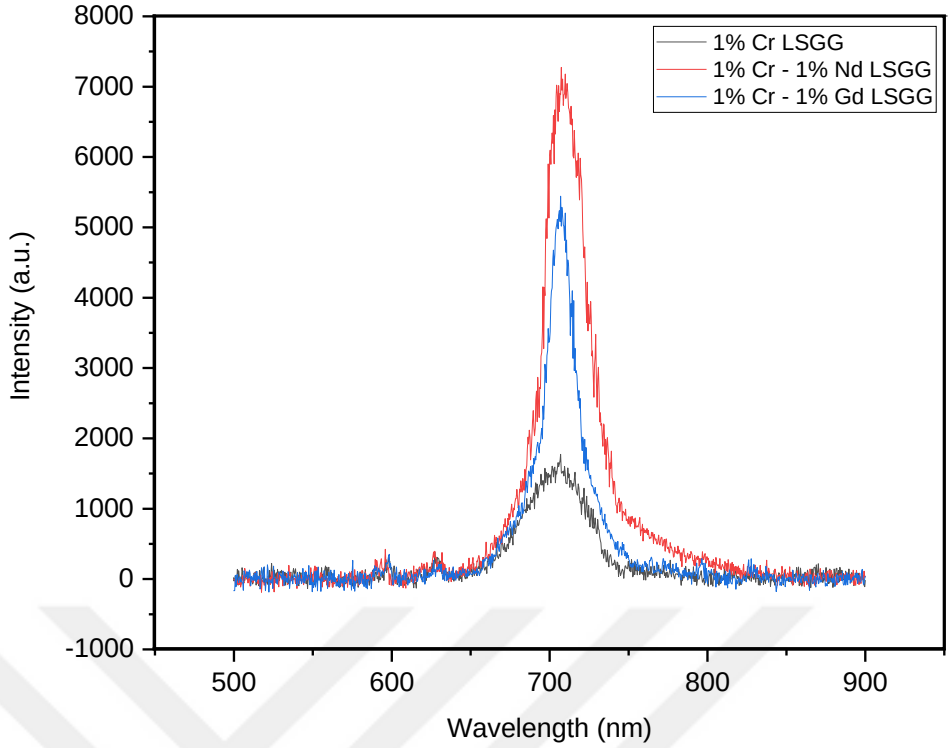


**Figure 5.9 :** Comparision of the afterglow properties of $Nd^{3+}$ and $Gd^{3+}$ co-doped $Sr^{2+}$ substituted phosphors.

In Figure 5.10, it was compared the decay curves of $Nd^{3+}$ and $Gd^{3+}$ co-doped samples of both substituted and non-substituted conditions.

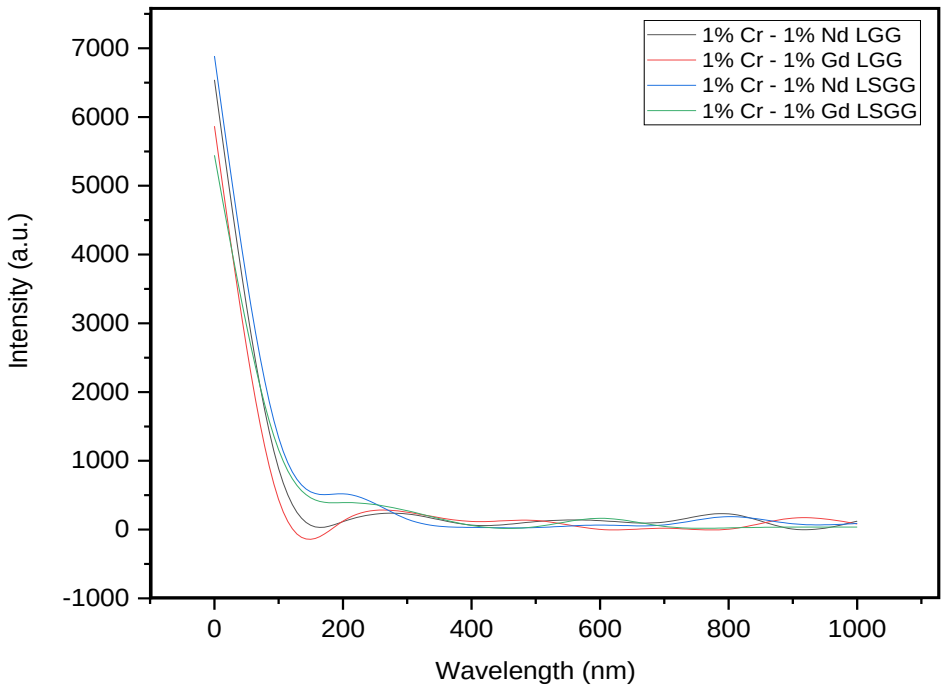


**Figure 5.10 :** Comparision of decay profiles of $Nd^{3+}$ and $Gd^{3+}$ co-doped LGG and LSGG phosphors.

From the decay curves, it has been understood that strontium substitution prolonged the afterglow duration in both co-dopant addition cases. This confirms that the structural defects are effective on prolonging the decay time as well as the traps created by co-dopants.

In Figure 5.11, afterglow intensities of $Nd^{3+}$ and $Gd^{3+}$ co-doped LGG and LSGG phosphors were compared separately for evaluating the change of emission wavelengths and intensities more clearly.

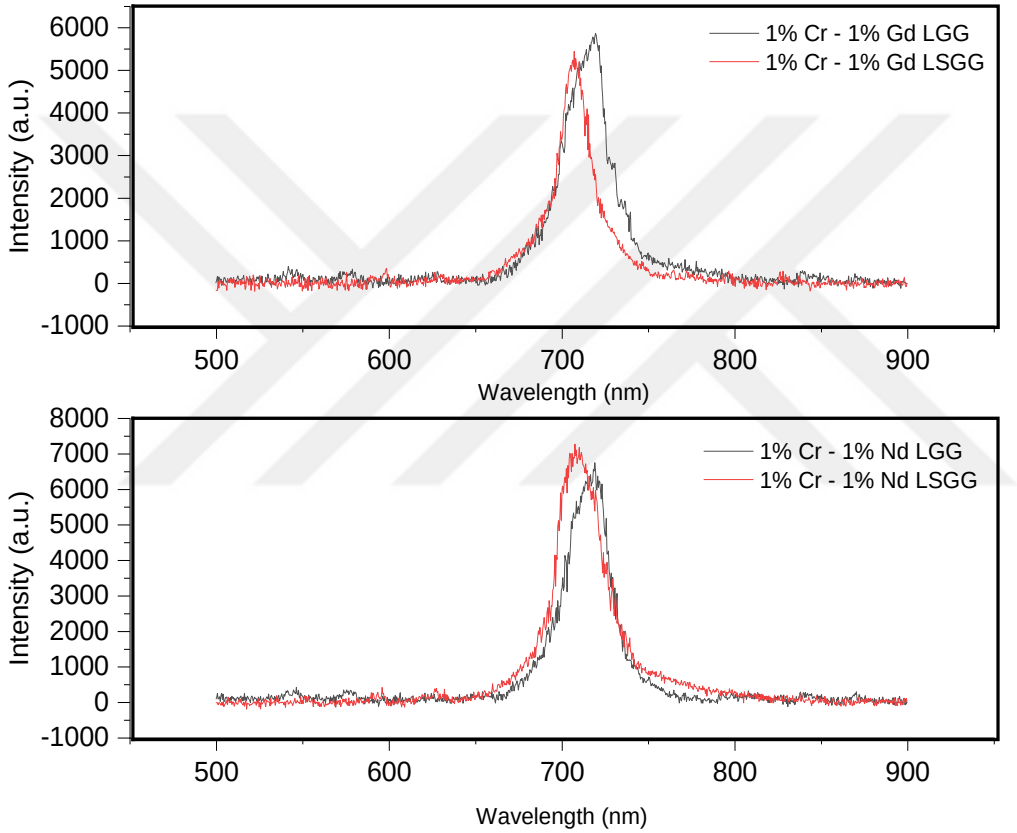


**Figure 5.11 :** Comparision of the afterglow properties of $Nd^{3+}$ and $Gd^{3+}$ co-doped LGG and LSGG phosphors.

According to the first graph, when LSGG sample was co-doped with $Gd^{3+}$, it was seen that the emission intensity decreases slightly compared to $Gd^{3+}$ co-doped LGG sample. On the contrary, co-doping with $Nd^{3+}$ ion increased the emission intensity of LSGG sample more than LGG. In both graphs, it was observed that the wavelength of the LSGG samples shifted to 709 nm from 719 nm.

In Figure 5.12, XRD patterns of all the strontium substituted and non-substituted samples were compared. The characteristics of the substituted samples were generally compatible with LGG structure and no changes in peak angles and positions detected.

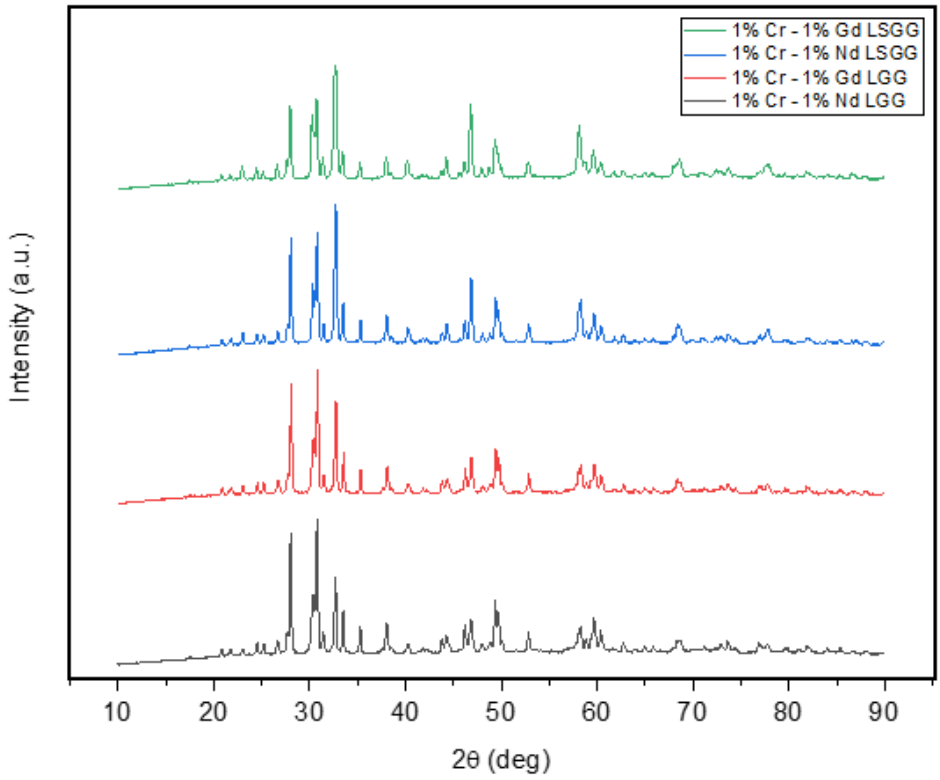


**Figure 5.12 :** XRD patterns of $Nd^{3+}$ and $Gd^{3+}$ co-doped LGG and LSGG phosphors.

### 5.4 Effects of $Ga^{3+}$ Substitution with $Al^{3+}$ and $Mg^{2+}$

In the previous steps of the experimental study, the optimum $Cr^{3+}$ doping rate, which contributed positively to the phosphorescent properties, the highest performance co-dopant and the optimum replacement rate of $La^{3+}$ with $Sr^{2+}$ were determinated. In the last step, $Al^{3+}$ and $Mg^{2+}$ ions were added to the $Ga^{3+}$ ion in the structure of $La_{2.8}Sr_{0.2}Ga_5GeO_{14}$: 1% Cr, 1% Nd separately and their effects on crystal structure and phosphorescence properties were examined. The reason for choosing Al and Mg as the substitution elements was that they have a similar ionic radius with the Ga ions in the structure. The final formulas of the samples were $La_{2.8}Sr_{0.2}Ga_4AlGeO_{14}$ and $La_{2.8}Sr_{0.2}Ga_4MgGeO_{14}$.

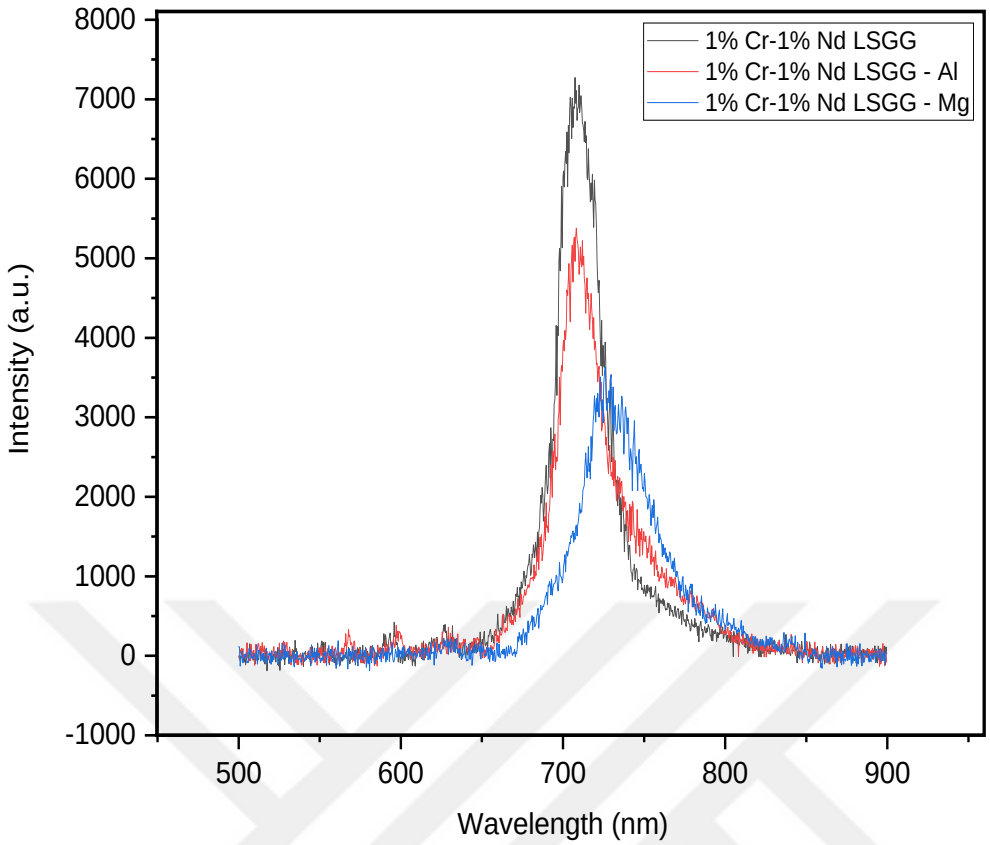


**Figure 5.13 :** Comparision of afterglow properties of $Al^{3+}$ and $Mg^{2+}$ substituted LSGG phosphors.

It was clearly seen in Figure 5.13 that the $Al^{3+}$ and $Mg^{2+}$ ions adding into the structure by replacement with a certain amount of $Ga^{2+}$ ion reduced the afterglow intensity. This might be resulted from the impurities caused by the free $Al^{3+}$ and $Mg^{2+}$ ions that are not included in the main structure. Besides, especially in the Mg substituted sample, emission wavelength has shifted forward from 709 to 726 nm and the shape of the emission peak broader than non-substituted LSGG. This means that the $Mg^{2+}$ substituted LSGG phosphor irradiates in the broader NIR spectrum with lower intensity. In the $Al^{3+}$ substitution case, emission characteristics and wavelentgh have been similar with the non-substituted LSGG sample; however, the emission intensity of the Al substitute sample has not been as much high as the non-substitute LSGG.

In Figure 5.14, decay profiles of the substituted samples were compared with the non-substitute LSGG according to the durations of the light emitting. Although the $Al^{3+}$ substitution reduced the afterglow intensity in this case, it has prolonged the decay time compared to other samples.

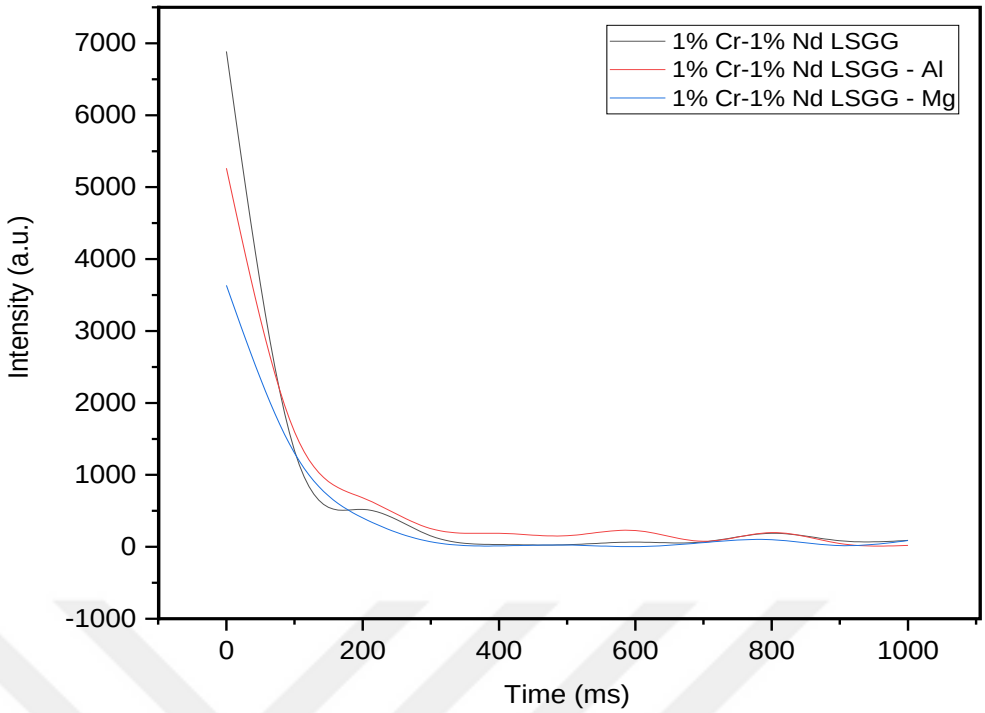


**Figure 5.14 :** Comparision of decay curves of $Al^{3+}$ and $Mg^{2+}$ substituted LSGGs.

As can be seen in Figure 5.15, there is a difference between XRD pattern of the $Mg^{2+}$ substituted sample and $Al^{3+}$ substituted and non-substituted LSGG samples' pattern. The changes in the peak angles of the $Mg^{2+}$ substituted sample explain the the differences in the emission wavelength, intensity and duration.

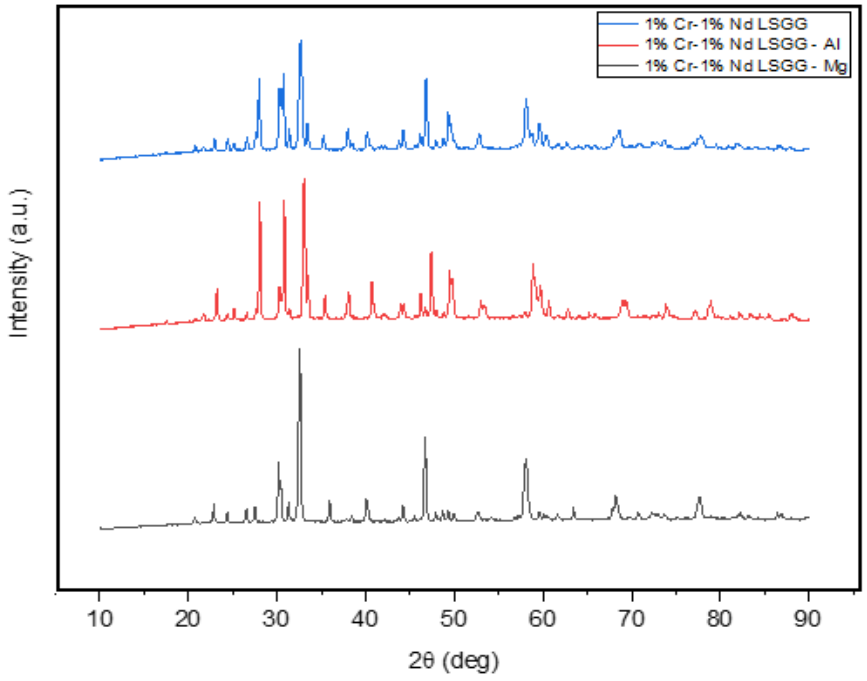


**Figure 5.15 :** XRD patterns of $Al^{3+}$ and $Mg^{2+}$ substituted LSGG phosphors.

# 6. CONCLUSIONS AND RECOMMENDATIONS

- In this study, lanthanum gallogermanate phosphors were synthesized using the sol-gel method unlike the studies about this type of phosphors in the literature.
- $Cr^{3+}$ was chosen as the main dopant owing to the fact that its ability to create luminescence centers in the structure. The crystal structures of the chromium doped LGG phosphors at different chromium concentrations were compared. Ratio of 1% has been determined as the optimum dopant dosage.
- According to the XRD results, phosphors calcined at 800 °C showed a crystal structure and proved to have phase of $La_3Ga_5GeO_{14}$ corresponding to JCPDS number of 00-72-2464. When co-dopants and substitution elements were added to the structure, a single phase was obtained and XRD patterns were compatible with the pattern of original phase structure.
- $Dy^{3+}$, $Nd^{3+}$, $Gd^{3+}$ and $Pr^{3+}$ were selected as the co-doping elements and they added to the system at the same ratio as $Cr^{3+}$, 1%. According to the optical measurements, $Nd^{3+}$ co-doped LGGC phosphors showed the best afterglow properties in terms of the emission intensity and decay time. Also in this case, the $Cr^{3+}$ doped and the co-doped gallogermanate phosphor samples have given sharp emission peaks at 719 nm.
- The effects of adding $Sr^{2+}$ at different ratios by replacing with $La^{3+}$ ions were also investigated. The highest emission intensity and the longest decay time were obtained with the case of $Nd^{3+}$ co-doped LGGC phosphor sample substituting with $Sr^{2+}$ at the ratio of 0.2. With the substitution, the emission wavelength has shifted to 709 nm from 719 nm.
- It has been determined that substituting $Ga^{3+}$ ions in the LSGG structure with $Al^{3+}$ and $Mg^{2+}$ ions decreases the emission intensity. In addition, unlike other LSGG samples, the emission wavelength has shifted to 726 nm in the case of $Mg^{2+}$ substitution, while the emission peak has become wider. It was also found

that the $Al^{3+}$ substitution affected positively to the decay profile of LSGG phosphor.

- The integration of $Sr^{2+}$, $Al^{3+}$ and $Mg^{2+}$ elements into the structure of $La_3Ga_5GeO_{14}$ phosphor and the effects of the co-doping with the rare earth elements such as $Nd^{3+}$, $Gd^{3+}$, $Pr^{3+}$ and $Dy^{3}$ have been investigated comprehensively in this study.

## REFERENCES


[1] **Goldberg, M. C., and Weiner, E. R.** (1989). Luminescence applications. *ACS Symposium Series,* American Chemical Society, Washington, DC.

[2] **Cheng, B., and Wang, Z.** (2005). Synthesis and optical properties of europium-doped ZnS: long-lasting phosphorescence from aligned nanowires, *Advanced Functional Materials, 15,* 1883-1890.

[3] **Matsuzawa, T., Aoki, Y., Takeuchi, N., and Murayama, Y.** (1996). A new long phosphorescent phosphor with high brightness, $SrAl_2O_4$:$Eu^{3+}$, $Dy^{3+}$, *Journal of the Electrochemical Society*, *143*(8), 2670-2673.

[4] **Eeckhout, K., Poelman, D., and Smet, P. F.** (2013). Persistent luminescence in non-Eu2+-doped compounds: A review, *Materials, 6,* 2789-2818.

[5] **Wang, Q., Zhang, S., Li, Z., and Zhu, Q.** (2018). Near infrared-emitting $Cr^{3+}$/$Eu^{3+}$ co-doped zinc gallogermanate persistence luminescent nanoparticles for cell imaging, *Nanoscale Research Letters,* 2-9.

[6] **Yen, M. W., Shionoya, S., and Yamamoto, H.** (2007). *Phosphor Handbook: Second Edition.* Florida, Taylor & Francis Group, LLC.

[7] **Feldmann, C., Jüstel, T., Ronda, C. R., and Schmidt, P. J.** (2003). Inorganic luminescent materials: 100 years of research and application, *Advanced Functional Materials, 13*(7), 511-516.

[8] **Anesh, M. P., Gulrez, S. Y. K. H., Anis, A., Shaikh, H., Mohsin, M. E. A., and Al-Zahrani, S. M.** (2014). Developments in Eu2+-doped strontium aluminate and polymer/strontium aluminate composite, *Advanced in Polymer Technology*, *33*(1), 21436.

[9] **URL-1** <*https://www.sas.upenn.edu/~mcnemar/firefly/fluor2.html*>, date retrieved 01.02.2019.

[10] **Yersin, H., Rausch, A. F., Czerwieniec, R., Hofbeck, T., and Fischer, T.** (2011). The triplet state of organo-transition metal compounds. Triplet harvesting and singlet harvesting for efficient OLEDs, *Coordination Chemistry Reviews, 255,* 2622-2652.

[11] **Fereja, T. H., Hymete, A., and Gunesekaran, T.** (2013). A recent review on chemiluminescence reaction, principle and application on pharmaceutical analysis, *Hindawi Publishing Corporation.* doi: 10.1155/2013/230858.

[12] **URL-2** <*http://www.sci.utah.edu/~macleod/bioen/be6003/labnotes/*>, date retrieved 12.02.2019.

[13] **Zimmermann, J., Zeug, A., and Röder, B.** (2003). A generalization of the Jablonski diagram to account for polarization and anisotropy effects in time-resolved experiments, *Physical Chemistry Chemical Physics, 5,* 2964-2969.

[14] **Uzun, E., and Yarar, Y. Y.** (2011). Modelling of thermoluminescence trap energy levels of Seydişehir alumuna, *Journal of Engineering and Natural Science, 29,* 25-34.

[15] **Wu, S, Pan, Z., Chen, R., and Liu, X.** (2017). *Long Afterglow Phosphorescent Materials.* Springer.

[16] **Ronda, C.** (2008). *Luminescence: From Theory to Applications.* Weimheim, Wiley-VCH.

[17] **Chen, C., and Chen, T.** (2001). Effect of host compositions on the afterglow properties of phosphorescent strontium aluminate phosphors derived from the sol-gel method, *Journal of Materials Research and Technology, 16*(5), 1293-1299.

[18] **Smet, P. F., Moreels, I., Hens, Z. and Poelman, D.** (2010). Luminescence in sulfides: A rich history and a bright future, *Electrochemical and Solid-State Letters, 13*(4), 2834-2883.

[19] **Jia, D., Lewis, L. A., and Wang, X.** (2010). $Cr^{3+}$-doped lanthanum gallogermanate phosphors with long persistent IR emission, *Materials, 3,* J32-J34.

[20] **Pan, Z., Lu, Y., and Liu, F.** (2012). Sunlight-activated long-persistent luminescence in the near-infrared from $Cr^{3+}$-doped zinc gallogermanates, *Nature Materials, 11,* 58-62.

[21] **Liu, C., Xia, Z., Molokeev, M. S., and Quanlin, L.** (2015). Synthesis, crystal structure, and enhanced luminescence of garnet-type $Ca_3Ga_2Ge_3O_{12}$:$Cr^{3+}$ by codoping $Bi^{3+}$, *Journal of American Ceramic Society, 98*(6), 1870-1876.

[22] **Wu, Y., Li, Y., Qin, X., Chen, R., Wu, D., Liu, S., and Qiu, J.** (2015). Dual mode NIR long persistent phosphorescence and NIR-to-NIR Stokes luminescence in $La_3Ga_5GeO_{14}$: $Cr^{3+}$, $Nd^{3+}$ phosphor, *Journal of Alloys and Compounds,* 1-6.

[23] **Zhou, J., and Xia, Z.** (2013). Synthesis and near-infrared luminescence of $La_3GaGe_5O_{16}$:$Cr^{3+}$ phosphors, *Royal Society of Chemicals Advances, 1*.

[24] **Dudka, A. P.** (2017). Multicell model of $La_3Ga_5GeO_{14}$ crystal: A new approach to the description of the short-range order of atoms, *Crystallography Reports, 62*(3), 374-381.

[25] **Li, Y., Gecevicius, M., and Qiu, J.** (2016). Long persistent phosphors: From fundamentals to applications, *Chemical Society Reviews.*

[26] **Ye, S., Song, E. H., Ma, E., Zhang, S. J., Wang, J., Chen, X. Y., Zhang, Q. Y., and Qiu, J. R.** (2014). Broadband Cr3+-sensitized upconversion luminescence in $La_3Ga_5GeO_{14}$: $Cr^{3+}$, $Yb^{3+}$, $Er^{3+}$, *Optical Materials Express, 4*(4), 639-648.

[27] **Yan, W., Liu, F., Lu, Y., Wang, X., Yin, M., and Pan, Z.** (2010). Near infrared long-persistent phosphorescence in $La_3Ga_5GeO_{14}$:$Cr^{3+}$ phosphor, *Optics Express, 18*(19), 20215-20220.

[28] **Levy, D., and Zayat, M.** (2015). *The Sol-Gel Handbook.* Wiley-VCH.

[29] **Brinker, C. J., and Scherer, G. W.** (1990). *Sol-Gel Science: The Physics and Chemistry of Sol-Gel Processng.* California, Academic Press, INC.

[30] **Macfarlane, P.I., Han, T.P.J., Henderson, B., and Kaminskii, A.A.** (1994). $Cr^{3+}$ luminescence in calcium and strontium gallogermanate, *Optical Materials, 3,* 15-24.

**CURRICULUM VITAE**

**Name Surname** **: Burcu CAN**

**Place and Date of Birth** **: Keşan, 19/09/1992**

**E-Mail** **: canbur@itu.edu.tr**

**EDUCATION** **:**

- **B.Sc.** **:** 2015, Istanbul Technical University, The Faculty of Chemical and Metallurgical Engineering, Chemical Engineering Department

**PROFESSIONAL EXPERIENCE AND REWARDS:**

- 2019 ECZACIBAŞI TUKETİM ÜRÜNLERİ – R&D Specialist
- 2017 ARTS ET MÉTIERS PARISTECH - Athens Exhange Student, Polymers and Composites Course
- 2015-2019 KASTAMONU ENTEGRE – R&D Engineer